Available online at www.sciencedirect.com
SCIENCE DIRECT®
Biochemical and Biophysical Research Communications 324 (2004) 697–704
BBRC
www.elsevier.com/locate/ybbrc

PPARα ligands activate antioxidant enzymes and suppress hepatic fibrosis in rats

Tetsuya Toyama, Hideki Nakamura, Yuichi Harano, Norihito Yamauchi, Atsuhiro Morita, Toshihiko Kirishima, Masahito Minami, Yoshito Itoh, Takeshi Okanoue*

Molecular Gastroenterology and Hepatology, Kyoto Prefectural University of Medicine, Graduate School of Medical Science, Kyoto, Japan

Received 8 September 2004

Abstract

Oxidative stress is a major pathogenetic factor in hepatic fibrosis. Peroxisome proliferator-activated receptor α (PPARα) is a nuclear receptor which is known to affect oxidative stress and PPARα ligands may have rescue effects on hepatic fibrosis. We tested this hypothesis using rat thioacetamide (TAA) models of liver cirrhosis. Rats were given intraperitoneal injection of TAA and treated with a diet containing one of the two PPARα ligands, Wy-14,643 (WY) or fenofibrate. WY treatment dramatically reduced hepatic fibrosis and also prevented the inhibition catalase of mRNA expression caused by TAA. Correspondingly, catalase activity increased in the TAA + WY group but decreased in the control TAA group. The antifibrotic action of fenofibrate in the TAA model was comparable with that of WY. PPARα ligands have an antifibrotic action in the rat TAA model of liver cirrhosis, probably due to an antioxidant effect of enhanced catalase expression and activity in the liver.

Keywords: Hepatic fibrosis; PPARα; Wy-14,643; Fenofibrate; Oxidative stress; Catalase; Hydrogen peroxide; Thioacetamide

Hepatic fibrosis is an inflammatory response to chronic hepatic damage due to viral infections, immunological insults, alcoholic damage, and other factors, and ultimately leads to liver cirrhosis and hepatic failure. Therefore, prevention and treatment of fibrosis is an important therapeutic goal in hepatology. Increased levels and altered nature of extracellular matrix (ECM) proteins due to the activation of hepatic stellate cells (HSCs) are thought to underlie hepatic fibrosis [1–3]. In hepatic fibrosis, HSCs have been reported to transform from the resting to active phenotype to secrete massive amounts of ECM proteins [3,4]. Oxidative stress also plays a role in hepatic fibrosis [5]. Reactive oxygen species (ROS), such as hydrogen peroxide (H_2O_2), act to promote liver fibrosis [5,6]. Accordingly, extrinsic H_2O_2 enhanced TGFβ-1 production in HSCs and catalase treatment blocked this effect [7].

Recently, peroxisome proliferator-activated receptor γ (PPARγ) ligands, such as thiazolidinediones (TZDs), were reported to prevent hepatic fibrosis in vitro and in vivo [15]. PPARs are ligand-activated transcription factors belonging to the nuclear hormone receptor superfamily and are involved in energy homeostasis [9]. Three PPAR isotypes, PPARα, PPARβ, and PPARγ, are found in most vertebrates, including humans and other mammals [10,11]. PPARγ is expressed abundantly in adipose tissue, moderately in the immune system [12], and to some extent in non-parenchymal cells in the liver [13,15]. However, the mechanisms for the antifibrotic actions of PPARγ remain unclear. In contrast, another isotype, PPARα, is distributed in

* Corresponding author. Fax: +81 75 251 0710.
E-mail address: okanoue@koto.kpu-m.ac.jp (T. Okanoue).

0006-291X/$ - see front matter © 2004 Elsevier Inc. All rights reserved.
doi:10.1016/j.bbrc.2004.09.110

metabolically active tissues including liver, most prominently in hepatocytes, as well as in kidney and heart [9,16,17]. The major action of PPARα is the regulation of fatty acid metabolism [17]. One class of PPARα ligands, the fibrates, has been used clinically to reduce triglyceride levels by suppressing the transcription of apo-C III acting as a lipoprotein lipase inhibitor, activating lipoprotein lipase, and lowering the concentration of total and very low density lipoprotein triglyceride [18].

Another action of PPARα is the upregulation of peroxisomes. Ligands such as fibrates and 4-chloro-6-(2,3-xylidino)-2-pyrymidinylthioacetic acid (Wy-14,643) are known to cause peroxisome proliferation and hepatomegaly in rodents [9]. Furthermore, fibrates were also reported to enhance superoxide dismutase (SOD) expression and catalase activity in the liver [14,19]. In light of the antioxidant actions, as well as the specific expression of the receptors in hepatocytes, we have hypothesized that PPARα ligands exert suppressive effects on hepatic fibrosis. We tested this hypothesis using the rat thioacetamide (TAA) model of liver cirrhosis and found that PPARα ligands, such as Wy-14,643 and fenofibrate, have a dramatic therapeutic effect on hepatic fibrosis probably via their antioxidant actions.

Materials and methods

Animal models. Male Wistar rats (Shimizu Experimental Materials, Kyoto, Japan) weighing 200 g were used in this study. Rats were allowed free access to water and laboratory chow. Rats in the TAA group received intraperitoneal (i.p.) injections of TAA (200 mg/kg body weight (BW) twice weekly; Wako Pure Chemical Industries, Osaka, Japan) for 6 weeks and rats in the Wy-14,643 treatment group were fed a diet containing 0.1% (w/w) Wy-14,643 (Tokyo Kasei Kogyo, Tokyo, Japan) during the entire experiment. They were divided into the following four groups: (i) those given a normal diet and i.p. injections of saline instead of TAA (control group) ($n = 6$); (ii) Wy-14,643-treatment and i.p. injections of saline instead of TAA (WY group) ($n = 6$); (iii) a normal diet and TAA-treatment (TAA group) ($n = 6$); and (iv) Wy-14,643-treatment and TAA-treatment (TAA+WY group) ($n = 6$). In addition, some rats ($n = 6$) were given i.p. injections of TAA (200 mg/kg) and fed a diet containing 0.1% (w/w) fenofibrate (Kaken Seiyaku, Tokyo, Japan) for 6 weeks. All procedures were performed according to experimental protocols approved by the Ethical Committee for Animal Experiments of Kyoto Prefectural University of Medicine.

Histopathologic examinations. Hematoxylin–eosin (HE) and Azan staining was performed, and serum samples and liver tissues were kept frozen at −80 °C until assayed. Semi-quantitative analyses of fibrotic areas were performed using a digital still camera system (Fujix Photograb-300Z SH-3Z; Fuji, Tokyo, Japan) and an NIH image-analyzing system five ocular fields (magnification 40×) per specimen for six rats per group.

Serum makers. Serum samples were obtained from the inferior cava vein and alanine aminotransferase (ALT) and hyaluronic acid levels were determined by routine laboratory methods.

Northern blot hybridization. Total RNA (20 μg per lane) was resolved by electrophoresis on a 1.2% agarose gel containing 2.2 M formaldehyde and transferred to a nylon membrane (Amersham Pharmacia Biotech, Piscataway, NJ) by capillary blotting. Hybridization was performed using a ^{32}P-labeled random-primed rat acyl-CoA oxidase (ACO), rat α1 (I) procollagen, rat CuZn–SOD, rat catalase, and rat glyceraldehyde-3-phosphate dehydrogenase (GAPDH) probes. The mRNA was quantitated by densitometry and normalized to the level of GAPDH.

Real-time quantitative reverse transcription-polymerase chain reaction (RT-PCR). Total RNA (2 μg) was reverse transcribed to cDNA with the Supersript First-Strand Synthesis System (Life Technologies, Gaithersburg, MD). Specific rat PPARα, TGF-β1, and GAPDH primers for real-time RT-PCR were obtained from Nihon Gene Research Laboratory (Sendai, Japan). Gene specific PCR products were quantitated by real-time RT-PCR with LightCycler (Roche, Mannheim, Germany). Reactions were prepared in 20-μl volumes using the LightCycler FastStart DNA Master SYBR Green I kit from Roche according to the manufacturer's protocol. The real-time PCR was analyzed by the second derived maximum algorithm and the results were normalized against the expression level of the internal control GAPDH.

Biochemical analyses. Rats were anesthetized with ether and their livers were cleared of blood by perfusion with 0.9% NaCl solution. Lipid peroxidation (LPO) products in the perfused liver, i.e., malondialdehyde (MDA), were estimated using an LPO-586 colorimetric kit (Oxis International, Portland OR). Reduced (GSH) and oxidized glutathione (GSSG) levels were measured in the perfused liver using commercially available kits (Bioxytech GSH-420, Oxis International; and Glutathione Assay Kit, Cayman Chemical, Ann Arbor, MI, respectively).

Determination of antioxidant enzyme activities. To determine CuZn–SOD activity of the perfused liver tissues, a spectrophotometric assay kit (Bioxytech SOD-525, Oxis International) was used according to the manufacturer's instructions. Catalase activity was measured using the spectrophotometric method of Beers and Sizer [20], and expressed as units/mg protein as described by Aebi [21].

Statistical analysis. Results are expressed as means ± SD. Statistical differences between means were determined using Student's t test and a one-way ANOVA (with appropriate post hoc analysis) for multiple comparisons. P values <0.05 were considered statistically significant.

Results

General effects of TAA and Wy-14,643 treatment

TAA models were selected as one of the most suitable experimental preparations for chronic liver injury and liver cirrhosis in humans [22].

Table 1 summarizes the general effects of single and combined treatments of TAA and Wy-14,643. No rats died during this experiment. There was a significant increase in liver weight (LW) and the LW/BW ratio in the WY and TAA + WY groups, and a slight increase in the TAA group (Table 1). The serum ALT level generally increased in the TAA and TAA + WY groups, indicating that Wy-14,643 did not ameliorate TAA hepatotoxicity. Conversely, there was a marked increase (64-fold) of the serum hyaluronic acid level in the TAA group, while the increase was more modest (10-fold) in the TAA + WY group relative to control, indicating that Wy-14,643 has a strong antifibrotic action.

Table 1
Effect of TAA and Wy-14,643 treatment on rat body weight, liver weight, and biochemical parameters

Groups		BW (g)	LW (g)	LW/BW (%)	ALT (IU/L)	Hyaluronic acid (ng/ml)
Controls	6 weeks	369.5 ± 6.0	12.4 ± 0.3	3.4 ± 0.1	51.8 ± 6.3	2.0 ± 1.9
WY	6 weeks	310.2 ± 6.6*,†	28.0 ± 1.5*,***	9.0 ± 0.3*,***	70.4 ± 11.4***	5.6 ± 4.0***
TAA	6 weeks	265.1 ± 12.2*	13.2 ± 0.9	5.0 ± 0.4**	185.2 ± 38.9*	127.0 ± 14.5*
TAA + WY	6 weeks	267.2 ± 16.8*	26.0 ± 2.6*,***	9.7 ± 0.8*,***	233.0 ± 36.4*	20.4 ± 5.6***

Note. Body and liver weights were recorded at the time of killing. ALT and hyarulonic acid were determined in venous blood samples obtained from the inferior cava vein after anesthesia and determined by the routine method used in the laboratory hospital. Data are expressed as the mean ± SD. BW, body weight; LW, liver weight.

* $P < 0.0001$ vs. controls.
** $P < 0.001$ vs. controls.
*** $P < 0.0001$ vs. TAA.
† $P < 0.05$ vs. TAA.

Wy-14,643 prevents TAA-induced hepatic fibrosis

Azan staining demonstrated marked fibrosis and signs of hepatic cirrhosis, such as centrilobular and periportal collagen deposition with fibrotic septa in the TAA group (Fig. 1C). Wy-14,643 treatment dramatically reduced the hepatic fibrosis in the TAA + WY group (Fig. 1D), and the histology in the WY group was similar to that in the control group (Figs. 1A and B). Correspondingly, computer-assisted semiquantitative analysis of fibrotic areas demonstrated a marked increase (31-fold) in the TAA group relative to control, and a rather slight increase (5.7-fold) in the TAA + WY group.

Expression of PPARα, TGF-β1, ACO, and collagen mRNAs

Real-time quantitative PCR of PPARα and densitometric analysis of Northern blotting of ACO

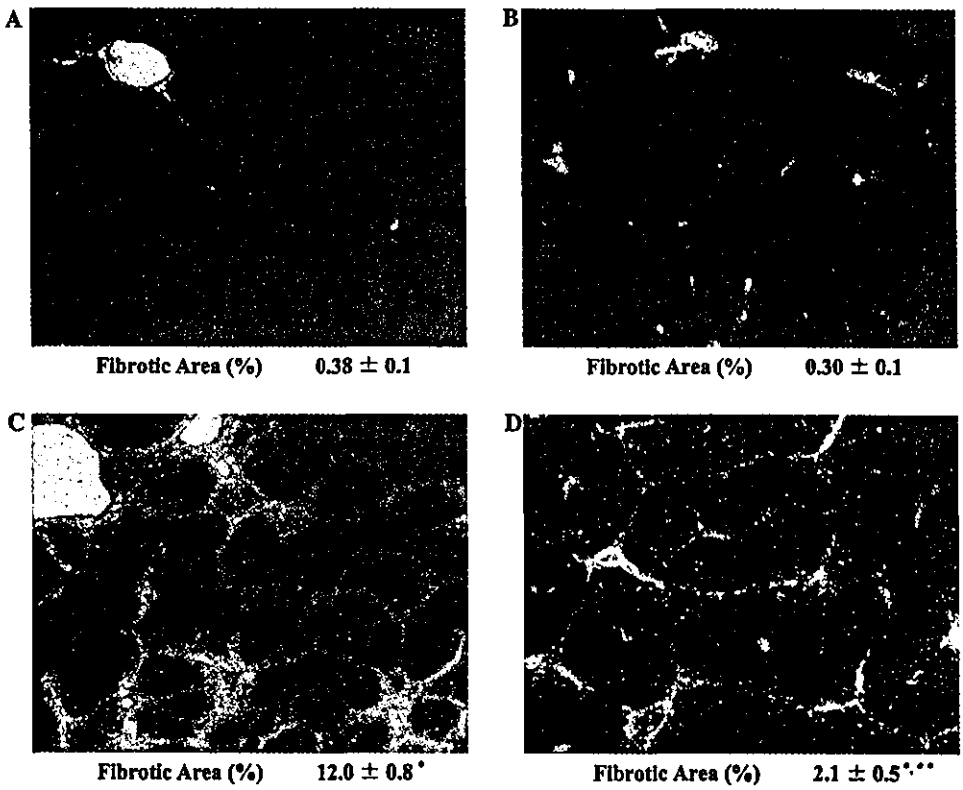

Fig. 1. Hepatic histology in four rat groups. (A–D) Photomicrographs of rat liver histology (Azan staining, original magnification, 40×). (A) Control group receiving 6-week treatment with saline, (B) 6-week treatment with Wy-14,643 (1 g/kg diet), (C) 6-week treatment with TAA (200 mg/kg BW), and (D) 6-week treatment with TAA + Wy-14,643. Fibrotic area is shown under each photograph. The signal positive area was quantitated by densitometric analysis of an NIH image. A total of five sections for each hepatic tissue sample were analyzed under 40× magnification. Figures represent the mean ± SD ($n = 6$). *$P < 0.0001$ or higher degree of significance vs. controls; $^{\dagger}P < 0.0001$ or higher degree of significance vs. TAA group.

confirmed that Wy-14,643 treatment activated PPARα by a striking increase in the mRNA for ACO which is one of the major target enzymes of PPARα in the WY and TAA + WY groups, and conversely no detectable expression was found in the TAA group (Figs. 2A, C, and D). A striking increase (14-fold) in the mRNA levels of α1 (I) procollagen in the TAA group was revealed, while the increase remained rather marginal (3.1-fold) in the TAA+WY group relative to the control group (Figs. 2E and F). Comparable changes were also found for mRNA levels of TGFβ-1 (Fig. 2B).

Expression and activity of hepatic antioxidant enzymes and oxidative stress markers

PPARα may activate antioxidant enzymes such as SOD and catalase [14,19]. This possibility was tested by Northern blotting and densitometric analysis of the mRNA expression for these enzymes in the perfused liver. Importantly, the mRNA level for catalase was markedly reduced (43% of control) in the TAA groups, while the mRNA level was increased over 3.8-fold (vs. control) both in the WY and TAA + WY groups (Figs. 3A and B). Therefore, Wy-14,643 enhanced catalase

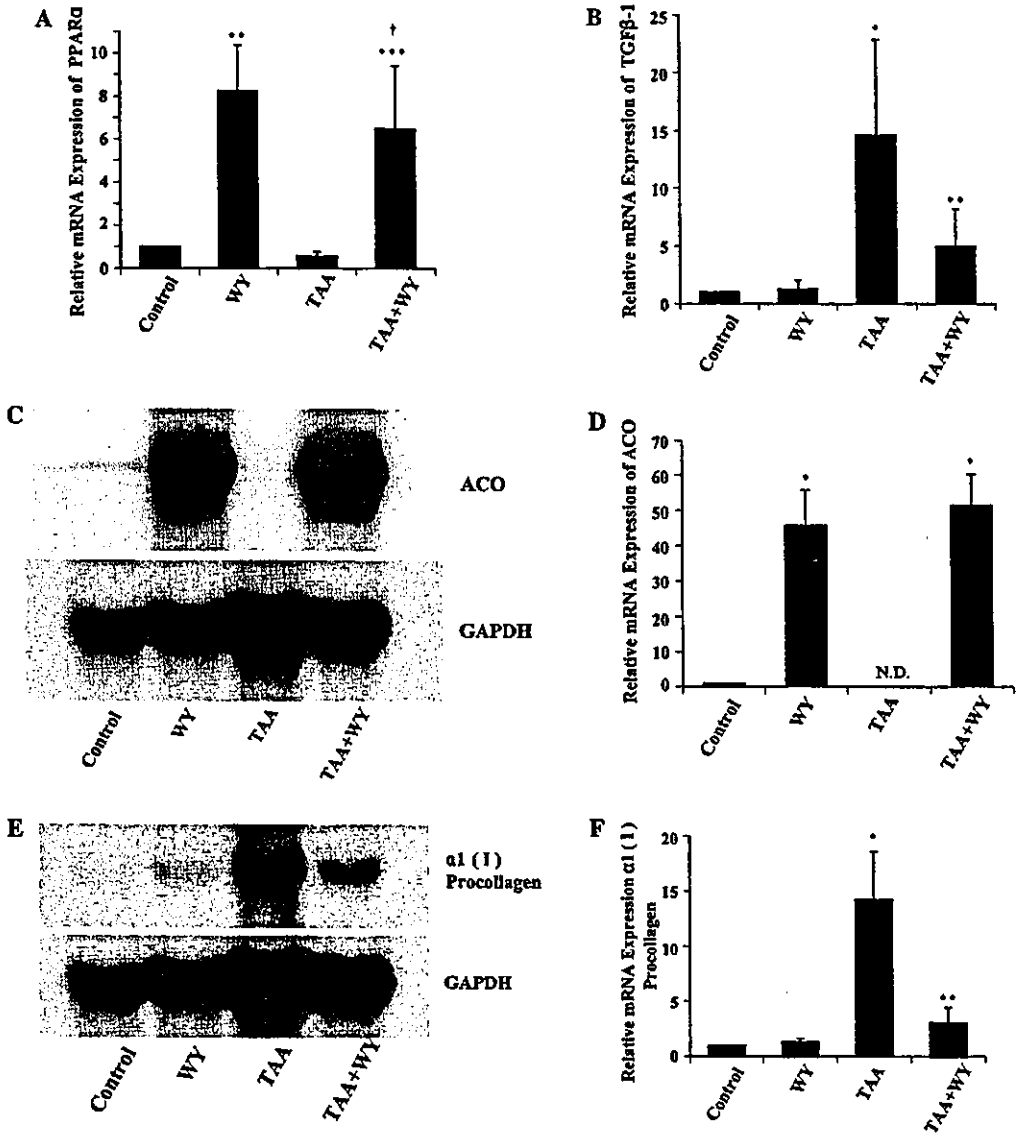

Fig. 2. mRNA expression of PPARα, TGF-β1, ACO, and α1 (I) procollagen in the liver of four rat groups. (A,B) Results of real-time quantitative PCR of PPARα and TGF-β1 mRNA for the four rat groups whose histologies are shown in Fig. 1, expressed as a ratio to GAPDH (mean ± SD for three different experiments performed in triplicate). (C,D) Photomicrographs of Northern blots for ACO mRNA and bar plots of densitometry for the four rat groups. The blot was then stripped and rehybridized with the rat GAPDH probe. (E,F) Photomicrographs of Northern blots for α1 (I) procollagen mRNA and corresponding bar plots of mRNA densitometry to (C) and (D). $^{*}P < 0.0001$ or higher degree of significance vs. controls; $^{\dagger}P < 0.001$ or higher degree of significance vs. controls; $^{\ddagger}P < 0.05$ or higher degree of significance vs. controls; $^{\S}P < 0.05$ or higher degree of significance vs. TAA groups; and ND, not detected.

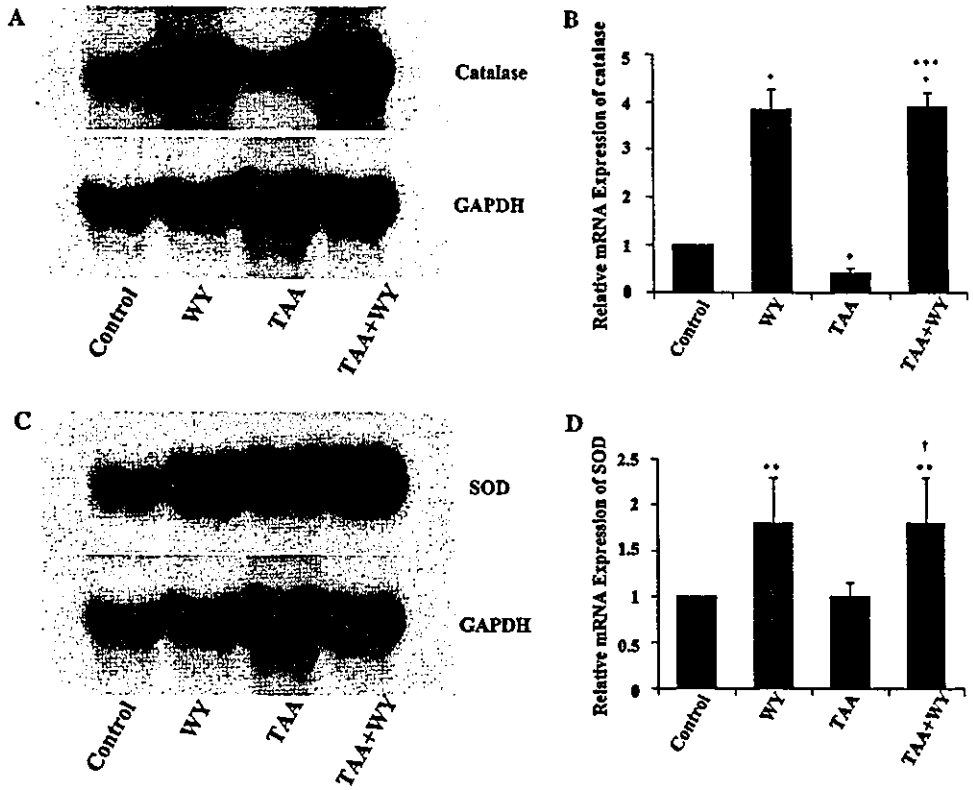

Fig. 3. mRNA densitometry for catalase and SOD in the liver of four rats groups. (A,B) Corresponding specimens and bar plots of mRNA densitometry to Figs. 2C and D for catalase, and (C,D) for SOD. $^{*}P < 0.0001$ or higher degree of significance vs. controls; $^{\dagger}P < 0.001$ or higher degree of significance vs. controls; $^{\ddagger}P < 0.0001$ or higher degree of significance vs. TAA groups; and $^{\S}P < 0.001$ or higher degree of significance vs. TAA groups.

expression and even reversed the suppression of catalase expression caused by TAA. Less striking and less specific enhancement effects of Wy-14,643 were observed on SOD mRNA expression. The mRNA expression remained at the control level in the TAA group and increased moderately (about 2-fold) in the WY and TAA + WY groups (Figs. 3C and D).

We also confirmed that levels of activity of antioxidant enzymes including catalase and SOD were increased following Wy-14,643 treatment. The effects of both TAA and Wy-14,643 were greater on catalase than on SOD activity. Catalase activity decreased markedly (36% of control) in the TAA group, and increased 2-fold in the WY and TAA + WY groups (Table 2). There was a comparable decrease in SOD activity (40%) in the TAA group but no change in the TAA + WY and WY groups. We also studied the effects of TAA and Wy-14,643 on the concentration

Table 2
Effect of TAA and Wy-14,643 treatment on antioxidative enzymes, glutathione levels, and LPO in the liver

Groups		GSH (μM/g tissue)	GSSG (μM/100 mg tissue)	SOD (U/mg protein)	Catalase (U/mg protein)	LPO (μM/100 mg tissue)
Controls	6 weeks	5.6 ± 0.4	74.7 ± 5.7	85.9 ± 8.8	141.5 ± 5.5	6.3 ± 1.4
WY	6 weeks	5.7 ± 1.0	$64.7 \pm 9.0^{\dagger}$	$72.7 \pm 11.4^{\ddagger}$	$278.0 \pm 14.1^{*,\dagger}$	$6.6 \pm 0.5^{\ddagger}$
TAA	6 weeks	6.8 ± 0.9	$212.2 \pm 30.5^{*}$	$35.0 \pm 6.1^{*}$	$51.7 \pm 5.0^{**}$	$11.6 \pm 0.7^{**}$
TAA + WY	6 weeks	6.5 ± 0.8	$140.0 \pm 33.3^{***}$	$72.1 \pm 9.3^{\ddagger}$	$279.0 \pm 14.9^{*,\dagger}$	$6.7 \pm 0.5^{\ddagger}$

Note. GSH and GSSG contents, the activities of SOD and catalase, and LPO were determined as desribed under Materials and methods. Data are expressed as the mean ± SD, $n = 6$.

* $P < 0.0001$ vs. controls.
** $P < 0.001$ vs. controls.
*** $P < 0.05$ vs. controls.
‡ $P < 0.001$ vs. TAA.
† $P < 0.0001$ vs. TAA.

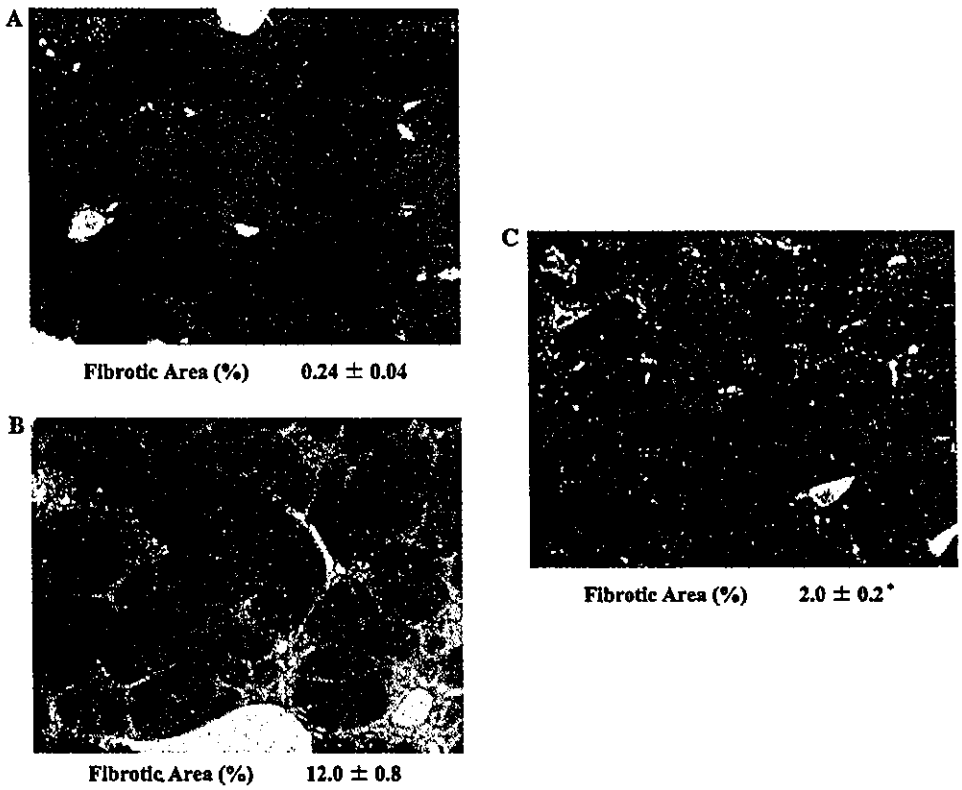

Fig. 4. Effect of fenofibrate on TAA-induced hepatic fibrosis. (A–C) Corresponding photomicrographs of liver histology to Figs. 1A–D. (A) Groups receiving 6-week fenofibrate, (B) 6-week TAA, and (C) 6-week TAA + fenofibrate treatment. Fibrotic area is shown under each photograph. Figures represent the mean ± SD ($n = 6$). *Significant differences ($P < 0.0001$) obtained by comparison between specimens for 6-week TAA and TAA + fenofibrate treatment.

of hepatic GSH and GSSG which are the substrate and product, respectively, of glutathione peroxidase, another major H_2O_2 reducing enzyme (cf. Fig. 5). There was a significant increase (2–3-fold) in the GSSG concentration in the TAA and TAA + WY groups, but no significant changes in the GSH concentration (Table 2), suggesting that the glutathione system might not be affected by Wy-14,643.

Finally, we investigated LPO in the liver. LPO roughly doubled in the TAA group and remained at the control value in the TAA + WY and WY groups (Table 2). These findings indicated that oxidative stress was increased by TAA treatment, and that this effect was reversed by Wy-14,643 treatment.

Fenofibrate also prevents TAA-induced hepatic fibrosis

Lastly, we investigated whether fenofibrate, which is a ligand of PPARα currently used therapeutically for hyperlipidemia, also has antifibrotic effects. We found that hepatic fibrosis was suppressed almost to the same extent (16% of the TAA group) in the group co-administered 0.1% fenofibrate (w/w) and TAA (200 mg/kg BW i.p.) for 6 weeks as in the TAA + WY group (Figs. 4A–C).

Discussion

Our study demonstrated that the PPARα ligand, Wy-14,643, has dramatic suppressive effects on TAA-induced hepatic fibrosis. A similar antifibrotic effect of Wy-14,643 was very recently reported for hepatic fibrosis induced by a methionine and choline deficient diet [30]. We hypothesize that hepatic cirrhosis is caused by a regenerative chain of events, such that hepatic damage increases oxidative stress, and activates HSCs, and the resulting fibrosis further worsens the oxidative stress. PPARα ligands may disrupt this vicious cycle by activating antioxidant enzymes such as catalase and resolving the oxidative stress (cf. Fig. 5). In support of this view, we found a close parallel between the hypothetical players of the antifibrotic actions of PPARα, including PPARα mRNA expression, catalase activity, LPO, and hepatic fibrosis under our experimental conditions. PPARα mRNA expression was reduced in the TAA group, which showed robust hepatic fibrosis, while expression was significantly increased in the TAA + WY group, which had virtually no fibrosis (Fig. 2A). There was also a dramatic reduction of catalase and SOD activity, and a robust increase in oxidative stress determined as LPO in the former group, and conversely there

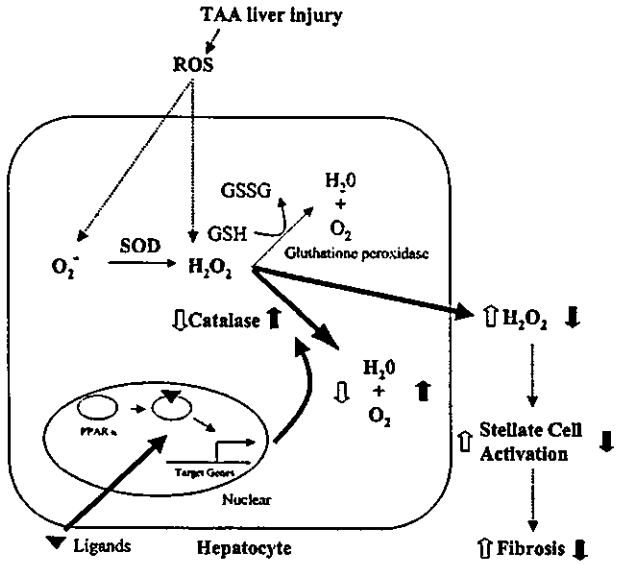

Fig. 5. Schematic diagram illustrating chemical pathways postulated for TAA-induced hepatic fibrosis and antifibrotic effects of PPARα ligands. Hepatic injury caused by TAA increases ROS, which is converted by SOD to H_2O_2. Normally, H_2O_2 is quickly removed by catalase in hepatocytes. Glutathione peroxidase may provide an additional pathway for the elimination of H_2O_2. Hepatic injury also impairs catalase expression as well as activity, elevates intracellular H_2O_2 and the extracellular H_2O_2 levels due to transmembrane permeation, and activates HSCs for fibrosis (open arrows). PPARα lignands suppress hepatic fibrosis by activating PPARα, enhancing catalase activity, reducing the extracellular H_2O_2, and inactivating HSCs (filled arrows). Thick and thin solid arrows indicate major and minor causal relationships postulated in the present study, and dotted arrows indicate an indirect causal relationship.

was a significant increase of catalase and SOD activity and no detectable increase in LPO in the latter group (Table 2). A similar dramatic reduction was found for catalase expression in the TAA group, but not in the TAA + WY group.

All of these findings are consistent with the view that hepatic injury impairs PPARα expression in hepatocytes, reduces catalase activity, and ultimately triggers the vicious cycle of hepatic fibrosis. The application of PPARα ligands is thought to compensate for the reduction in PPARα expression and prevent the cycle of hepatic fibrosis. Importantly, we found almost the same reduction in catalase mRNA expression and activity in the 4 week TAA-treated rats, in which hepatic fibrosis remained prodromal (data not shown), as that for the 6 week TAA group, in which the fibrosis was established (Table 2). This finding suggests that the impairment of catalase activity is the cause rather than a consequence of TAA-induced hepatic fibrosis. Thus, the increase in oxidative stress caused by impaired catalase activity may be a key element in triggering hepatic fibrosis.

In support of this view, levels of ROS were reported to increase in response to hepatic damage, such as that caused by hepatic iron overload, ethanol intoxication, or aging [5,24]. We point to H_2O_2 among the ROS as a major agent triggering hepatic fibrosis, since it easily permeates the cellular membrane, acting as an intercellular messenger [5,25]. In fact, H_2O_2 was found to activate TGFβ-1 and collagen production by HSCs [7,8]. Catalase may be the most relevant enzyme involved in detoxification of H_2O_2 and protection of hepatocytes from oxidative stress [7]. Catalase is contained in peroxisomes and is involved in eliminating H_2O_2 produced by fatty acid β-oxidation [26]. There are several studies reporting the relevance of catalase to hepatic fibrosis: i.e., catalase blocked TGFβ-1 and collagen production in HSCs [7], catalase activity was reduced in human hepatic injury and cirrhosis [23,27], and overexpression of catalase rescued hepatic damage [31]. The peroxisome proliferator response element (PPRE), the binding site for PPAR, has been recently identified in the promoter area for the catalase gene [28], and therefore, catalase has been identified as one of the target enzymes of PPARα. Moreover, PPARα is predominantly expressed in hepatocytes rather than in hepatic non-parenchymal cells such as HSCs [13,15,29]. Fig. 5 summarizes the pharmacological mechanisms that we postulate for the antifibrotic action of PPARα. Liver injury caused by TAA increases ROS levels and impairs PPARα expression and catalase activity in hepatocytes. Catalase is a major pathway for the elimination of intracellular H_2O_2 produced by SOD, while glutathione peroxidase also acts as an additional pathway for detoxifying H_2O_2. The impairment of catalase activity elevates the intracellular levels of H_2O_2, which can permeate cellular membranes and diffuse extracellularly where it acts on HSCs to promote fibrosis (blank arrows). PPARα ligands activate catalase, resulting in a decrease in extracellular H_2O_2 levels and prevention of fibrosis by HSC activation (filled arrows).

It is very unlikely that the antifibrotic effect of Wy-14,643 was due to its hepatoprotective action, since the hepatic damage, estimated by serum ALT levels and a histological examination conducted in the acute phase, revealed a similar extent of hepatocyte necrosis(data not shown), implying that Wy-14,643 treatment did not reverse the acute hepatic damage caused by TAA. Furthermore, we also found that fenofibrate, which is one of the PPARα ligands currently used as a hypolipidemic agent, exhibited comparable antifibrotic effects to Wy-14,643 (Fig. 4). This finding points to the possibility of using PPARα ligands as antifibrotic therapeutics for hepatic disease.

In conclusion, our study demonstrated that PPARα ligands including Wy-14,643 and fenofibrate exert dramatic antifibrotic action on TAA-induced hepatic fibrosis, probably through antioxidant actions on hepatocytes. Our results indicate that fenofibrate, which is currently used in therapy of hyperlipidemia, may be a useful new therapy for treating fibrosis and can be used as an antifibrotic agent acting on hepatocytes in con-

junction with other agents acting on HSCs, such as angiotensin-II type 1 receptor blocker [32].

References

[1] E. Olaso, S.L. Friedman, Molecular regulation of hepatic fibrogenesis, J. Hepatol. 29 (1998) 836–847.

[2] M. Rojkind, M.A. Giambrone, L. Biempica, Collagen types in normal and cirrhotic liver, Gastroenterology 76 (1979) 710–719.

[3] S. Milani, H. Herbst, D. Schuppan, E.G. Hahn, H. Stein, In situ hybridization for procollagen types I, III and IV mRNA in normal and fibrotic rat liver: evidence for predominant expression in nonparenchymal liver cells, Hepatology 10 (1989) 84–92.

[4] S.L. Friedman, Seminars in medicine of the Beth Israel Hospital, Boston. The cellular basis of hepatic fibrosis. Mechanisms and treatment strategies, N. Engl. J. Med. 328 (1993) 1828–1835.

[5] M. Parola, G. Robino, Oxidative stress-related molecules and liver fibrosis, J. Hepatol. 35 (2001) 297–306.

[6] G. Poli, Pathogenesis of liver fibrosis: role of oxidative stress, Mol. Aspects Med. 21 (2000) 49–98.

[7] P.J. De Bleser, G. Xu, K. Rombouts, V. Rogiers, A. Geerts, Glutathione levels discriminate between oxidative stress and transforming growth factor-beta signaling in activated rat hepatic stellate cells, J. Biol. Chem. 26 (274) (1999) 33881–33887.

[8] G. Svegliati Baroni, L. D'Ambrosio, G. Ferretti, A. Casini, A. Di Sario, R. Salzano, et al., Fibrogenic effect of oxidative stress on rat hepatic stellate cells, Hepatology 27 (1998) 720–726.

[9] I. Issemann, S. Green, Activation of a member of the steroid hormone receptor superfamily by peroxisome proliferators, Nature 347 (1990) 645–650.

[10] C. Dreyer, G. Krey, H. Keller, F. Givel, G. Helftenbein, W. Wahli, Control of the peroxisomal beta-oxidation pathway by a novel family of nuclear hormone receptors, Cell 68 (1992) 879–887.

[11] S.A. Kliewer, B.M. Forman, B. Blumberg, E.S. Ong, U. Borgmeyer, D.J. Mangelsdorf, et al., Differential expression and activation of a family of murine peroxisome proliferator-activated receptors, Proc. Natl. Acad. Sci. USA 91 (1994) 7355–7359.

[12] K.L. Houseknecht, C.A. Bidwell, C.P. Portocarrero, M.E. Spurlock, Expression and cDNA cloning of porcine peroxisome proliferator-activated receptor gamma (PPARgamma), Gene 28 (225) (1998) 89–96.

[13] J.M. Peters, I. Rusyn, M.L. Rose, F.J. Gonzalez, R.G. Thurman, Peroxisome proliferator-activated receptor alpha is restricted to hepatic parenchymal cells, not Kupffer cells: implications for the mechanism of action of peroxisome proliferators in hepatocarcinogenesis, Carcinogenesis 21 (2000) 823–826.

[14] J. Berger, D.E. Moller, The mechanisms of action of PPARs, Annu. Rev. Med. 53 (2002) 409–435.

[15] A. Galli, D.W. Crabb, E. Ceni, R. Salzano, T. Mello, G. Svegliati-Baroni, et al., Antidiabetic thiazolidinediones inhibit collagen synthesis and hepatic stellate cell activation in vivo and in vitro, Gastroenterology 122 (2002) 1924–1940.

[16] O. Braissant, F. Foufelle, C. Scotto, M. Dauca, W. Wahli, Differential expression of peroxisome proliferator-activated receptors (PPARs): tissue distribution of PPAR-alpha, -beta, and -gamma in the adult rat, Endocrinology 137 (1996) 354–366.

[17] K. Schoonjans, M. Watanabe, H. Suzuki, A. Mahfoudi, G. Krey, W. Wahli, et al., Induction of the acyl-coenzyme A synthetase gene by fibrates and fatty acids is mediated by a peroxisome proliferator response element in the C promoter, J. Biol. Chem. 270 (1995) 19269–19276.

[18] S.M. Grundy, G.L. Vega, Fibric acids: effects on lipids and lipoprotein metabolism, Am. J. Med. 83 (1987) 9–20.

[19] I. Inoue, S. Noji, T. Awata, K. Takahashi, T. Nakajima, M. Sonoda, T. Komoda, et al., Bezafibrate has an antioxidant effect: peroxisome proliferator-activated receptor alpha is associated with Cu2+, Zn2+-superoxide dismutase in the liver, Life Sci. 63 (1998) 135–144.

[20] R.F. Beers, I.W. Sizer, A spectrophotometric method for measuring the breakdown of H_2O_2 by catalase, J. Biol. Chem. 195 (1952) 133–140.

[21] H. Aebi, Catalase in vitro, Methods Enzymol. 105 (1984) 121–126.

[22] E.M. Torres, J.I.P. Bouza, A.L. Bravo, M.M.A. Hernadez, E.C. Marino, Experimental thioacetamide-induced cirrhosis of the liver, Histol. Histopathol. 6 (1991) 95–100.

[23] H. Togashi, H. Shinzawa, H. Wakabayashi, T. Nakamura, N. Yamada, T. Takahashi, et al., Activities of free oxygen radical scavenger enzymes in human liver, J. Hepatol. 11 (1990) 200–205.

[24] G. Poli, M. Parola, Oxidative damage and fibrogenesis, Free Radic. Biol. Med. 22 (1997) 287–305.

[25] P.J. De Bleser, T. Niki, V. Rogiers, A. Geerts, Transforming growth factor-beta gene expression in normal and fibrotic rat liver, J. Hepatol. 26 (1997) 886–893.

[26] A. Schmidt, N. Endo, S.J. Rutledge, R. Vogel, D. Shinar, G.A. Rodan, Identification of a new member of the steroid hormone receptor superfamily that is activated by a peroxisome proliferator and fatty acids, Mol. Endocrinol. 6 (1992) 1634–1641.

[27] A. Pastor, P.S. Collado, M. Almar, J. Gonzalles-Gallego, Antioxidant enzyme status in biliary obstructed rats; effects of *N*-acetylcysteine, J. Hepatol. 27 (1997) 363–370.

[28] G.D. Girnun, F.E. Domann, S.A. Moore, M.C. Robbins, Identification of a functional peroxisome proliferator-activated receptor response element in the rat catalase promoter, Mol. Endocrinol. 16 (2002) 2793–2801.

[29] K. Hellemans, L. Michalik, A. Dittie, A. Knorr, K. Rombouts, J. De Jong, et al., Peroxisome proliferator-activated receptor-beta signaling contributes to enhanced proliferation of hepatic stellate cells, Gastroenterology 124 (2003) 184–201.

[30] E. Ip, G. Farrell, P. Hall, G. Robertson, I. Leclercq, Administration of the potent PPARα agonist, Wy-14,643, reverses nutritional fibrosis and steatohepatitis in mice, Hepatology 39 (2004) 1286–1296.

[31] J. Bai, A.I. Cederbaum, Adenovirus-mediated overexpression of catalase in the cytosolic or mitochondrial compartment protects against cytochrome P450 2E1-dependent toxicity in HepG2 cells, J. Biol. Chem. 230 (2001) 4315–4321.

[32] H. Yoshiji, S. Kuriyama, J. Yoshii, Y. Ikenaka, R. Noguchi, R. Noguchi, et al., Angiotensin-II type 1 receptor interaction is a major regulator for liver fibrosis development in rats, Hepatology 34 (2001) 745–750.

Characteristics of Patients with Chronic Hepatitis C who Develop Hepatocellular Carcinoma after a Sustained Response to Interferon Therapy

Akiko Makiyama, M.D.[1]
Yoshito Itoh, M.D., Ph.D.[1]
Akinori Kasahara, M.D., Ph.D.[2]
Yasuharu Imai, M.D., Ph.D.[3]
Sumio Kawata, M.D., Ph.D.[4]
Kentaro Yoshioka, M.D., Ph.D.[5]
Hirohito Tsubouchi, M.D., Ph.D.[6]
Kendo Kiyosawa, M.D., Ph.D.[7]
Shinichi Kakumu, M.D., Ph.D.[8]
Kiwamu Okita, M.D., Ph.D.[9]
Norio Hayashi, M.D., Ph.D.[10]
Takeshi Okanoue, M.D., Ph.D.[1]

[1] Molecular Gastroenterology and Hepatology, Kyoto Prefectural University of Medicine, Graduate School of Medical Science, Kyoto, Japan.

[2] Department of General Medicine, Osaka University Graduate School of Medicine, Suita, Japan.

[3] Department of Internal Medicine, Ikeda Municipal Hospital, Osaka, Japan.

[4] Second Department of Internal Medicine, Yamagata University, Yamagata, Japan.

[5] Third Department of Medicine, Nagoya University Graduate School of Medicine, Nagoya, Japan.

[6] Second Department of Internal Medicine, Miyazaki Medical College, Miyazaki, Japan.

[7] Second Department of Medicine, Shinsyu University School of Medicine, Matsumoto, Japan.

[8] Department of Internal Medicine, Division of Gastroenterology, Aichi Medical University School of Medicine, Aichi, Japan.

[9] Department of Gastroenterology, Yamaguchi University School of Medicine, Yamaguchi, Japan.

[10] Department of Molecular Therapeutics, Osaka University Graduate School of Medicine, Osaka, Japan.

Supported in part by a grant 13670544 from the Ministry of Health, Labor, and Welfare, Japan.

Address for reprints: Takeshi Okanoue, M.D., Molecular Gastroenterology and Hepatology, Kyoto Prefectural University of Medicine, Graduate School of Medical Science, Kawaramachi-Hirokouji, Kamigyou-ku, Kyoto, 602-8566, Japan; Fax: 011 (81) 752510710; E-mail: tokanoue@sun.kpu-m.ac.jp

Received October 17, 2003; revision received May 7, 2004; accepted June 21, 2004.

BACKGROUND. The objective of the current study was to determine the characteristic features of sustained responders who develop hepatocellular carcinoma after treatment with interferon for chronic hepatitis C.

METHODS. This study included 3626 patients with chronic hepatitis C who had received interferon monotherapy. Cox proportional hazards analysis was used to compare sustained responders who did and did not develop hepatocellular carcinoma, and nonsustained responders who developed hepatocellular carcinoma in a multicenter, retrospective cohort study.

RESULTS. Among 1197 sustained responders, 27 patients developed hepatocellular carcinoma (2.3%). Compared with sustained responders who did not develop hepatocellular carcinoma, patients who developed disease more often were male ($P = 0.0212$), were older ($P = 0.0068$), and had advanced-stage histologic disease before interferon therapy ($P = 0.0345$). Conversely, compared with patients with hepatocellular carcinoma who were not sustained responders, patients who were sustained responders tended to be older at the time of the initiation of interferon therapy ($P = 0.0552$) and at the time hepatocellular carcinoma was detected ($P = 0.0593$), and they also were predominantly male ($P = 0.0507$). The histologic staging and serum aminotransferase levels at the initiation of interferon therapy, the interval to the detection of tumor, and the tumor size showed no significant differences between the two groups.

CONCLUSIONS. Sustained responders in the group at high risk for developing hepatocellular carcinoma after interferon therapy were older, more often were male, and had more advanced histologic disease stage. Such patients should be followed carefully periodically for > 10 years after they complete interferon therapy. *Cancer* 2004;101:1616–22. © *2004 American Cancer Society.*

KEYWORDS: chronic hepatitis type C, hepatocellular carcinoma, interferon, sustained responder.

In Japan, chronic hepatitis C (CH-C) with advanced histologic staging often progresses to hepatocellular carcinoma (HCC),[1] although patients who are seropositive for antihepatitis C virus (anti-HCV) antibodies or for HCV RNA do not always progress to cirrhosis or HCC.[2,3] Risk factors for developing HCC in patients with CH-C are advanced histologic stage, irregular regeneration of hepatocytes, heavy drinking, higher serum alanine aminotransferase (ALT) levels or lower serum albumin levels, male gender, and older age.[1,4–7] Since 1992, patients with CH-C commonly have been treated with interferon α (IFN-α) or IFN-β, which are covered by public health insurance in Japan. Because IFN improves hepatic inflammation and inhibits the progression of hepatic fibrosis, it

DOI 10.1002/cncr.20537
Published online 18 August 2004 in Wiley InterScience (www.interscience.wiley.com).

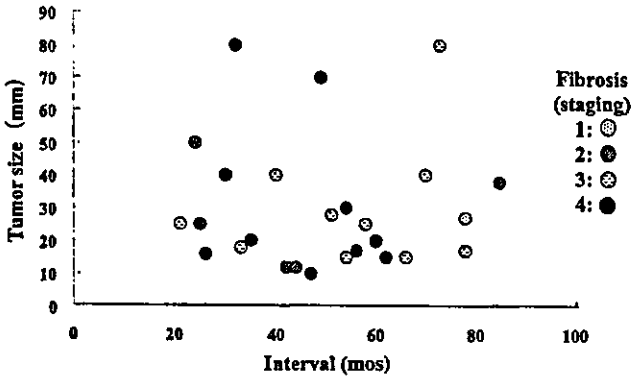

FIGURE 1. The interval from the completion of IFN therapy to the detection of SR HCC statistically did not correlate significantly with the tumor size or hepatic staging.

TABLE 1
Characteristics of Patients with Chronic Hepatitis C who were Treated with Interferon[a]

Characteristic	Sustained responder	Nonsustained responder	P value[b]
No. patients	1197	2429	—
Male:female ratio	776:421	1568:861	0.8826
Age (yrs, mean ± SD)	49.4 ± 11.9	51.2 ± 10.6	< 0.0001
Histologic staging score: No. of patients (%)			
F1	385 (38.6)	522 (25.8)	
F2	322 (32.3)	613 (30.3)	< 0.0001
F3	262 (26.3)	782 (38.6)	
F4	29 (2.9)	109 (5.4)	
Not available	199	403	

SD: standard deviation; IFN: interferon.
[a] All data were determined before interferon therapy.
[b] P values were calculated with the Fisher exact probability test and the Wilcoxon two-sample test.

has been suggested that the incidence of HCC may be reduced by IFN treatment. In fact, IFN therapy reportedly was effective not only for improving liver biochemistry and eliminating HCV RNA but also for reducing the inflammation/fibrosis scores and lowering the risk of HCC, especially in sustained responders (SR patients).[8–14]

Although a significant decrease in the incidence of HCC has been observed in SR patients after IFN therapy,[9–14] HCC is detected in some of them.[15–25] The clinical features of SR patients who develop HCC (SR HCC patients) and the long-term incidence of HCC in SR patients remain unclear, and the optimal duration and frequency of follow-up have not been established. Therefore, we analyzed SR HCC patients to determine their characteristic features compared with SR patients who did not develop HCC (SR non-HCC patients) and non-SRs who developed HCC (non-SR HCC patients).

MATERIALS AND METHODS

Patients

For this study, 3626 patients with CH-C were enrolled (2344 males and 1282 females) who had received IFN therapy between January 1990 and November 2001. Data from these patients were collected from 6 institutions and related hospitals, including 1371 patients from Kyoto Prefectural University of Medicine, 1478 patients from Osaka University, 497 patients from Miyazaki Medical College, 130 patients from Nagoya University, 102 patients from Shinsyu University, and 48 patients from Yamaguchi University. All patients were seropositive for anti-HCV antibodies, positive for serum HCV RNA, and seronegative for hepatitis B virus surface antigen. We excluded patients who had coexisting liver diseases, such as autoimmune hepatitis or primary biliary cirrhosis, and confirmed that they did not abuse alcohol (daily alcohol intake > 60 g of ethanol). No patients were infected with human immunodeficiency virus (HIV). At the time of entry into this study, no patients showed evidence of HCC, as determined by ultrasonography (US) and/or computed tomography (CT) studies. In principle, patients underwent liver biopsy prior to IFN therapy, and the histologic diagnoses were reached according to the classification of Desmet et al.[26] The gender, mean age, and histologic disease stage at the initiation of IFN therapy are shown in Table 1.

Natural IFN-α, recombinant IFN-α-2a, and recombinant IFN-α-2b were used in this study. In general, the IFN treatment protocol was within the range covered by public health insurance in Japan, namely, 3–10 MU of IFN-α for 24 weeks (daily for 2 weeks and 3 times per week for 22 weeks). In a few patients, administration of IFN-α was prolonged to 52 weeks. In some patients who suffered from severe side effects, the therapy period was shortened. In addition, patients for whom the total dose of IFN was < 200 MU were excluded from the study. Patients who had been treated with peginterferon or IFN/Ribavirin also were excluded. There was no difference noted with regard to the treatment protocol among the institutions and their related hospitals. We checked the laboratory findings at the end of IFN therapy and 6 months later. SR patients were defined as those who demonstrated continuous normal serum ALT levels for 6 months after finishing IFN therapy. The remaining patients were regarded as non-SR patients. The patient population included 1197 SR patients and 2429 non-SR patients.

We followed all patients for at least 1 year after the end of IFN therapy. The mean ± standard deviation

(SD) follow-up was 5.9 years ± 1.9 years. In SR patients, in general, we performed biochemical examinations, which sometimes included α-fetoprotein, every 3–12 months after confirming a sustained response. US and/or CT studies were performed at least once annually. However, because the incidence of HCC in non-SR patients—especially those with advanced-stage disease (fibrotic scores of F3 or F4)–was expected to be higher than that in SR patients, US and/or CT studies were performed every 3–6 months in non-SR patients. This strategy was similar in all of the institutions, and the frequency of radiographic examination was calculated to avoid unnecessary cost and not to miss HCC. However, some SR patients and non-SR patients who skipped or stopped visiting the outpatient clinic and some patients who were followed by their home physicians were not followed sufficiently. The diagnosis of HCC was based on appropriate radiologic findings (hepatic angiography, dynamic CT, magnetic resonance imaging).[27] When it was difficult to determine a final diagnosis with the radiologic findings, a histologic diagnosis was reached by tumor biopsy. In 17 of 27 SR HCC patients, a histologic diagnosis of HCC was obtained by the examination of resected hepatic tumors or biopsied tumor specimens. Patients who were diagnosed with HCC within 1 year after the end of IFN therapy were excluded from this study because of the possibility that a small but detectable HCC was missed before IFN therapy. Written informed consent to receive IFN therapy and to participate in this follow-up study was obtained from all patients, and the ethical committees of the participating institutions approved this study.

Statistical Analysis

Statistical analysis was performed using the SAS/PC statistical package (SAS Institute, Cary, NC). The Fischer exact probability test was used to compare the frequencies of gender. The Wilcoxon two-sample test was used to compare age, histologic staging, serum ALT level, interval between the end of IFN therapy and the detection of HCC, and the size of HCC. The independent risk factors for developing HCC in SR patients were examined by Cox proportional-hazards analysis; the variables were gender, age, histologic stage, and serum ALT level. Patients who had missing data were excluded from this analysis. Each variable was transformed into categorical data comprised of two-sample, ordinal numbers for multivariate analysis. P values were two-sided, and P values < 0.05 were considered statistically significant.

RESULTS

Characteristic Features of SR HCC Patients

During the observation of 3626 patients, HCC was detected in 259 patients; however, 19 patients were excluded, because HCC was detected within 1 year after they completed IFN therapy. The distribution of the remaining 240 HCC patients among the 6 institutions was as follows: 109 patients from Kyoto Prefectural University of Medicine (HCC incidence, 8.0%), 102 patients from Osaka University (HCC incidence, 6.9%), 3 patients from Miyazaki Medical College (HCC incidence, 0.6%), 15 patients from Nagoya University (HCC incidence, 11.5%), 8 patients from Shinsyu University (HCC incidence, 7.8%), and 3 patients from Yamaguchi University (HCC incidence, 6.3%). The incidence of HCC did not differ significantly among the institutions, except for Miyazaki Medical College. partly because hepatic fibrosis was less advanced in patients from this institution compared with patients from the other five institutions. Of 240 patients, 27 were SR patients, and 213 were non-SR patients. The ages of the 240 patients at the initiation of IFN therapy ranged from 37–77 years (mean age ± SD, 59.1 years ± 6.6 years) and varied from 39–83 years (63.6 years ± 6.8 years) at the time HCC was detected.

Among the 27 SR HCC patients, 5 patients consumed ≈ 50 g of ethanol daily. By evaluating liver specimens and biochemical examinations, including γ-glutamyl transferase, we excluded the possibility of alcoholic liver diseases in these patients. Serum HCV RNA was evaluated in the SR HCC patients by reverse transcriptase-polymerase chain reaction analysis. Twenty-six SR HCC patients were complete responders (seronegative for HCV RNA both at the end of IFN therapy and 6 months later), and 1 SR HCC patient was a biochemical responder (seropositive for HCV RNA at the end of IFN therapy). In 1 complete responder who developed HCC, serum HCV RNA became positive 12 months after completing IFN therapy.

No correlation could be found between the interval before HCC was detected, tumor size, or hepatic histologic stage among the SR HCC patients (Fig. 1). HCC that was detected long after discontinuing IFN therapy was not always large, and the patients with large HCC did not always show more advanced stage according to liver histology. The greatest dimensions of the 2 largest SR HCC tumors were 80 mm and were detected 32 months and 73 months after the end of IFN therapy. The greatest dimension of SR HCC found after the longest interval (85 months) was 38 mm.

Tumor tissue samples could be examined from 18 of 27 SR HCC patients. Two samples were categorized

TABLE 2
Comparisons between Sustained Responders with and without Hepatocellular Carcinoma[a]

Characteristic	SR HCC	SR non-HCC	*P* value[b]
No. of patients	27	1170	
Male:female ratio	25:2	751:419	0.0016
Age (yrs, mean ± SD)	60.7 ± 7.5	50.2 ± 12.4	< 0.0001
Serum ALT (IU/L, mean ± SD)	111.7 ± 67.7	122.6 ± 109.9	0.7267
Histologic staging score: No. of patients (%)			
F1	1 (3.7)	384 (39.6)	
F2	11 (40.7)	310 (32.0)	< 0.0001
F3	10 (37.0)	252 (26.0)	
F4	5 (18.5)	24 (2.5)	

SR: sustained responder; HCC: hepatocellular carcinoma; SD: standard deviation; ALT: alanine aminotransferase; IFN: interferon.

[a] All data were determined before interferon therapy.

[b] *P* values were calculated with the Fisher exact probability test and the Wilcoxon two-sample test.

TABLE 3
Factors Associated with the Development of Hepatocellular Carcinoma in Sustained Responders[a]

Characteristic	Risk ratio	95% CI	*P* value
Male vs. female	5.498	1.290–23.439	0.0212
Age	7.378	1.737–31.326	0.0068
Stage of liver disease	2.344	1.064–5.164	0.0345
Serum ALT	1.331	0.606–2.923	0.4768

95% CI: 95% confidence interval; ALT: alanine aminotransferase.

[a] All data were determined before interferon therapy. Statistical analysis was performed using the Cox proportional hazards test. The variable for age was set at < 50 years or ≥ 50 years, the variable for stage was set < F3 or ≥ F3, and the variable for the serum alanine aminotransferase level was set at < 88 UI/L or ≥ 88 UI/L. The variables age and serum alanine aminotransferase level were determined as median data. The variable for stage was set to obtain the largest hazard ratio.

as well differentiated HCC, 11 samples were moderately differentiated HCC, 2 samples were poorly differentiated HCC, and 2 samples were undifferentiated HCC. One sample was the necrotic tissue after transcatheter arterial embolization therapy (TAE). Nontumorous liver tissue samples from 18 patients were evaluated for their fibrosis scores in resected HCC or tumor biopsy specimens. Liver fibrosis scores improved in nine patients, did not change significantly in eight patients, and worsened in one patient.

Sixteen of 27 SR HCC patients underwent partial hepatectomy, and 10 patients were treated with TAE and/or percutaneous ethanol injection therapy. Because one patient changed his hospital after the diagnosis of HCC, we could not know his prognosis.

Comparison between SR HCC Patients and SR Non-HCC Patients

We compared 27 SR HCC patients with 1170 SR non-HCC patients. The SR HCC patients included 25 males (92.6%) and 2 females (7.4%), and the SR non-HCC patients included 751 males (63.5%) and 419 females (35.8%). At the time IFN therapy was initiated, the mean age of the SR HCC patients was 60.7 years ± 7.5 years (range, 37–70 years), whereas the mean age of the SR non-HCC patients was 50.2 years ± 12.4 years (range, 17–73 years). Thus, the SR HCC patients more often were male ($P = 0.0016$) and were older ($P < 0.0001$) compared with the SR non-HCC patients (Table 2).

The fibrotic scores in biopsied liver specimens before IFN therapy for the SR HCC patients included 1 F1 specimen (3.7%), 11 F2 specimens (40.7%), 10 F3 specimens (37.0%), and 5 F4 specimens (18.5%); and the fibrotic scores for the SR non-HCC patients included 384 F1 specimens (39.6%), 310 F2 specimens (32.0%), 252 F3 specimens (26.0%), and 24 F4 specimens (2.5%). The 2 female SR HCC patients both had F4 specimens. Among the total SR population, SR HCC patients had more advanced-stage disease ($P < 0.0001$). The mean serum ALT level at the initiation of IFN therapy was 111.7 IU/L ± 67.7 IU/L in the SR HCC patients and 122.6 IU/L ± 109.9 IU/L in the SR non-HCC patients (Table 2).

Cox proportional-hazards analysis of factors associated with the development of HCC in the SR patients was performed with four variables (gender, age, histologic stage, and serum ALT level). In this analysis, the hazard ratios for age, stage, and serum ALT level were calculated between the two groups. The age variable was set at < 50 years or ≥ 50 years, the fibrotic score (stage) variable was set at < F3 or ≥ F3, and the variable for serum ALT level was set at < 88 IU/L or ≥ 88 IU/L. The variables age and serum ALT level were determined as median data. We chose the variable for stage to obtain the greatest hazard ratio. The SR HCC patients more often were male ($P = 0.0212$, 95%CI, 1.290–23.439), were older ($P = 0.0098$, 95%CI, 1.737–31.326), and had advanced-stage disease according to liver histology ($P = 0.0345$; 95%CI, 1.064–5.164) before IFN therapy. Gender, age, and histologic stage before IFN therapy were considered independent risk factors for the development of HCC (Table 3).

Comparison between SR HCC Patients and Non-SR HCC Patients

We compared the clinical characteristics of the 27 SR HCC patients with the 213 non-SR HCC patients. The non-SR HCC patients included 161 males (75.6%) and 52 females (24.4%). The mean age of the non-SR HCC patients at the initiation of IFN therapy was 58.9 years ± 6.5 years (range, 40–77 years), and the mean age at

TABLE 4
Comparisons between Sustained Responders and Nonsustained Responders among Patients with Hepatocellular Carcinoma

Characteristic	SR	Non-SR	P value[a]
No. of patients	27	213	
Male:female ratio	25:2	161:52	0.0507
Age at the initiation of IFN (yrs, mean ± SD)	60.7 ± 7.5	58.9 ± 6.5	0.0552
Age at the detection of HCC (yrs, mean ± SD)	65.1 ± 7.8	63.4 ± 6.7	0.0593
Serum ALT (IU/L)[b]	111.7 ± 67.7	120.5 ± 56.4	0.2027
Histologic staging score: No. of patients (%)[b]			
F1	1 (3.7)	12 (5.6)	
F2	11 (40.7)	36 (16.9)	0.1861
F3	10 (37.0)	135 (63.4)	
F4	5 (18.5)	30 (14.1)	
Interval (mos, mean ± SD)[c]	49.3 ± 18.2	49.7 ± 24.8	0.7484
Tumor size (mm, mean ± SD)	31.2 ± 20.1	21.3 ± 9.9	0.1573

SR: sustained responder; IFN: interferon; SD: standard deviation; HCC: hepatocellular carcinoma; ALT: alanine aminotransferase.
[a]P values were calculated with the Fisher exact probability test and the Wilcoxon two-sample test.
[b]Data were determined before interferon therapy.
[c]The interval was between the completion of interferon therapy and the detection of hepatocellular carcinoma.

time HCC was detected was 63.2 years ± 6.7 years (range, 44–83 years). The mean serum ALT level in the non-SR HCC patients at the start of IFN therapy was 120.5 IU/L ± 56.4 IU/L. The fibrotic scores of biopsied liver specimens obtained from the non-SR HCC patients before IFN therapy included 12 F1 specimens (5.6%), 36 F2 specimens (16.9%), 135 F3 specimens (63.4%), and 30 F4 specimens (14.1%). Thus, concerning gender and age, the SR HCC patients tended to be predominantly male ($P = 0.0507$) and were older (both at the initiation of IFN therapy [$P = 0.0552$] and at the time HCC was detected [$P = 0.0593$]) compared with the non-SR HCC patients; however, the serum ALT levels and the histologic stage before IFN therapy among the SR HCC patients did not differ significantly compared with the non-SR HCC patients (Table 4).

The mean interval between the end of IFN therapy and the detection of HCC for the SR HCC patients was 49.3 months ± 18.2 months (range, 21–85 months), which was not significantly different from that for the non-SR HCC patients (49.7 months ± 24.8 months; range, 12–141 months). The mean greatest dimension of SR HCC was 31.2 mm ± 20.1 mm, which was slightly greater than, but not significantly different from, the mean greatest dimension of non-SR HCC (21.3 mm ± 9.9 mm) (Table 4).

DISCUSSION

In the current study, we compared the clinical characteristics of SR HCC patients with the characteristics of SR non-HCC patients to determine the characteristic features of SR HCC. The incidence of HCC among the 1197 SR patients was 2.3%, and the incidence among the 2429 non-SR patients was 8.8% during the mean follow-up of 5.9 years. In patients with CH-C, aging and advanced hepatic histologic stage reportedly are major risk factors for HCC development.[1,4] This was true for the SR population in our current investigation, because the risk ratio for developing HCC was > 7 times greater in older patients (≥ 50 years) and was more than twice as high in patients who had advanced histologic stage disease (fibrotic score ≥ F3) according to a Cox proportional-hazards analysis. Khan et al. also reported that male gender is an important risk factor for HCC development.[5] In the current study, males were more than five times more likely to develop HCC in the SR population. Thus, older male patients with advanced hepatic fibrosis were considered to be a high-risk group for developing HCC among the SR population (Table 3).

Conversely, compared with the non-SR HCC patients, the SR HCC patients were older at the initiation of IFN therapy ($P = 0.0552$) and at the detection of HCC ($P = 0.0593$), and they were predominantly male ($P = 0.0507$). Although these characteristics may not have differed significantly in the current study, a study of even larger size may show that this indeed is a trend. The histologic staging, the serum ALT level at the initiation of IFN therapy, the interval for the detection of HCC, and the tumor size did not differ significantly between the two groups. The tumor size in SR HCC patients was slightly greater compared with the tumor size in non-SR HCC patients, most likely because of the extended interval of screening for HCC after patients attained a sustained response to IFN therapy (Table 4).

Some previous articles reported that HCV RNA may survive in the hepatic tissues of SR HCC patients[28–30] and may be involved in the carcinogenesis or growth of HCC. Although we could not demonstrate the presence of HCV RNA in tumors and surrounding hepatic tissues from SR HCC patients, eradication of HCV from these tissues, along with the nontumorous hepatic tissues, was confirmed in several previous studies,[15–21] suggesting that the persistence of HCV is not essential for the growth of HCC in SR patients.

To ascertain the time of HCC occurrence, several studies were performed that examined the doubling time (DT) of HCC. Two studies from Japan reported that the DT of HCC measuring < 3 cm in greatest dimension was 93.0 days ± 57.4 days or 195.0 days ± 171.0 days.[31,32] Barbara et al. reported that the DT of HCC measuring < 5 cm in greatest dimension was 204.2 days ± 135 days.[33] Recently, Toyoda et al. re-

ported similar results, assuming that the greatest dimension of occult HCC was 5 mm before IFN therapy.[34] We calculated the growth interval between a single HCC cell and an HCC measuring 1 cm in greatest dimension on the assumption that the DT of HCC was 90 days and concluded that the growth interval may be > 6 years.[8] Because smaller and well differentiated HCCs have a longer DT, the growth interval to reach 1 cm in greatest dimension may be much longer than 6 years. Therefore, it is probable that small HCC may have existed in the liver prior to IFN therapy in the current SR HCC patients.[35]

It cannot be determined with certainty how long SR patients should be followed after they complete IFN therapy. Judging from the results obtained in the current study, we recommend that, when SR patients are male, age > 50 years old, and have F3 or F4 histologic stage, they should be checked by US or CT at least twice per year for > 10 years. Other SR patients with less advanced disease should be checked at least once per year.

REFERENCES

1. Ikeda K, Saitoh S, Suzuki Y, et al. Disease progression and hepatocellular carcinogenesis in patients with chronic viral hepatitis: a prospective observation of 2215 patients. *J Hepatol.* 1998;28:930–938.
2. Kenny-Walsh E, for the Irish Hepatology Research Group. Clinical outcomes after hepatitis C infection from contaminated anti-D immune globulin. *N Engl J Med.* 1999;340: 1228–1233.
3. Alberti A, Noventa F, Benvegnu L, Boccato S, Gatta A. Prevalence of liver disease in a population of asymptomatic persons with hepatitis C virus infection. *Ann Intern Med.* 2002;17:961–964.
4. Aizawa Y, Shibamoto Y, Takagi I, et al. Analysis of factors affecting the appearance of hepatocellular carcinoma in patients with chronic hepatitis C. A long term follow-up study after histologic diagnosis. *Cancer.* 2000;89:53–59.
5. Khan MH, Farrell GC, Byth K, et al. Which patients with hepatitis C develop liver complications? *Hepatology.* 2000; 31:513–520.
6. Shibata M, Morizane T, Uchida T, et al. Irregular regeneration of hepatocytes and risk of hepatocellular carcinoma in chronic hepatitis and cirrhosis with hepatitis-C-virus infection. *Lancet.* 1998;351:1773–1777.
7. Kasahara A, Hayashi N, Mochizuki K, et al. Clinical characteristics of patients with chronic hepatitis C showing biochemical remission, without hepatitis C eradication, as a result of interferon therapy. The Osaka Liver Disease Study Group. *J Viral Hepatol.* 2000;7:343–351.
8. Okanoue T, Itoh Y, Minami M, et al. Interferon therapy lowers the rate of progression to hepatocellular carcinoma in chronic hepatitis C but not significantly in an advanced stage: a retrospective study in 1148 patients. *J Hepatol.* 1999; 30:653–659.
9. Kasahara A, Hayashi N, Mochizuki K, et al. Risk factors for hepatocellular carcinoma and its incidence after interferon treatment in patients with chronic hepatitis C. Osaka Liver Disease Study Group. *Hepatology.* 1998;27:1394–1402.
10. Okanoue T, Itoh Y, Kirishima T, et al. Transient biochemical response in interferon therapy decreases the development of hepatocellular carcinoma for five years and improves the long-term survival of chronic hepatitis C patients. *Hepatol Res.* 2002;23:62–77.
11. Yoshida H, Shiratori Y, Moriyama M, et al. Interferon therapy reduces the risk for hepatocellular carcinoma: national surveillance program of cirrhotic and noncirrhotic patients with chronic hepatitis C in Japan. *Ann Intern Med.* 1999;131: 174–181.
12. Imai Y, Kawata S, Tamura S, et al. Relation of interferon therapy and hepatocellular carcinoma in patients with chronic hepatitis C. *Ann Intern Med.* 1998;129:94–99.
13. Ikeda K, Saitoh S, Arase Y, et al. Effect of interferon therapy on hepatocellular carcinogenesis in patients with chronic hepatitis type C: long-term observation study of 1,643 patients using statistical bias correction with proportional hazard analysis. *Hepatology.* 1999;29:1124–1130.
14. Tanaka H, Tsukuma H, Kasahara A, et al. Effect of interferon therapy on the incidence of hepatocellular carcinoma and mortality of patients with chronic hepatitis C: a retrospective cohort study of 738 patients. *Int J Cancer.* 2000;87:741–749.
15. Hirashima N, Mizokami M, Orito E, et al. Development of hepatocellular carcinoma in a patient with chronic hepatitis C infection after a complete and sustained response to interferon-alpha. *J Gastroenterol Hepatol.* 1996;11:955–958.
16. Inoue M, Ohhira M, Ohta T, et al. Hepatocellular carcinoma developed in a patient with chronic hepatitis C after the disappearance of hepatitis C virus due to interferon therapy. *Hepatogastroenterology.* 1999;46:2554–2560.
17. Miyano S, Togashi H, Shinzawa H, et al. Case report: occurrence of hepatocellular carcinoma 4.5 years after successful treatment with virus clearance for chronic hepatitis C. *J Gastroenterol Hepatol.* 1999;14:928–930.
18. Tamori A, Kuroki T, Nishiguchi S, et al. Case of hepatocellular carcinoma in the caudate lobe detected after interferon caused disappearance of hepatitis C virus. *Hepatogastroenterology.* 1996;43:1079–1083.
19. Kim SR, Matsuoka T, Maekawa Y, et al. Development of multicentric hepatocellular carcinoma after completion of interferon therapy. *J Gastroenterol.* 2002;37:663–668.
20. Okamura K, Yamazaki K, Ohmura T, et al. A resected case of hepatocellular carcinoma with sustained response to interferon for five years. *Acta Hepatol Jpn.* 2000;41:43–47.
21. Yamada M, Ichikawa M, Matsubara A, Ishiguro Y, Yamada M, Yokoi S. Development of small hepatocellular carcinoma 80 month after clearance of hepatitis C virus with interferon therapy. *Eur J Gastroenterol Hepatol.* 2000;12:1029–1032.
22. Nagano K, Fukuda Y, Nakano I, et al. A case of the development of two hepatocellular carcinoma and a cholangiocarcinoma with cirrhosis after elimination of serum hepatitis C virus RNA with interferon therapy. *Hepatogastroenterology.* 2000;47:1436–1438.
23. Sugo H, Kitayama N, Iwata T, et al. Development of hepatocellular carcinoma in a patients with chronic hepatitis C after a complete response to interferon therapy. *Acta Hepatol Jpn.* 2000;41:195–198.
24. Sugiura N, Sakai Y, Ebara M, et al. Detection of hepatocellular carcinoma after interferon therapy for chronic hepatitis C: clinical study of 26 cases. *J Gastroenterol Hepatol.* 1996;11:535–539.

Available online at www.sciencedirect.com
SCIENCE DIRECT®
Biochemical and Biophysical Research Communications 322 (2004) 1052–1058
BBRC
www.elsevier.com/locate/ybbrc

Chemokine CCL20 enhances the growth of HuH7 cells via phosphorylation of p44/42 MAPK in vitro

Hideki Fujii, Yoshito Itoh*, Kanji Yamaguchi, Norihito Yamauchi, Yuichi Harano, Tomoki Nakajima, Masahito Minami, Takeshi Okanoue

Graduate School of Medical Science, Molecular Gastroenterology and Hepatology, Kyoto Prefectural University of Medicine, Kyoto, Japan

Received 7 July 2004

Abstract

CCR6 is the receptor of chemokine CCL20. In the present study, we demonstrated that the surface expression of CCR6 was enhanced on the human HCC cell lines (HuH7, PLC/PRF/5, and HepG2) especially on HuH7 cells, but not on HLE or HLF cells. These HCC cell lines (HuH7, PLC/PRF/5, and HepG2) especially the HuH7 cells secreted a significant amount of CCL20 spontaneously, whereas HLE or HLF did not. Stimulation by CCL20 up-regulated the mRNA expression of CCR6 in HuH7 cells and significantly enhanced the growth of HuH7 cells. CCL20-stimulated growth of HuH7 cells was abrogated by the inhibition of downstream signal transduction pathway mediated by p44/42 MAPK, but not by p38 MAPK or SAPK/JNK. CCR6 expression in human HCC tissues was confirmed by RT-PCR. These results indicate that the growth of a proportion of human HCC cells may be mediated by CCL20–CCR6 axis, like HuH7 cells, in an autocrine or paracrine manner.

Keywords: HuH7; CCR6; CCL20; p44/42 MAPK

Chemokines are a family of low-molecular-weight, cytokine-like proteins that were initially defined as soluble chemotactic factors that direct the migration of leukocytes to inflammatory sites. They are divided into four subfamilies based on the cysteine residue in their NH_2-terminal region, and more than 50 chemokines have been identified. The secreted chemokines bind to seven-transmembrane, G-protein-coupled receptors on the surface of target cells to exert their biological activity [1,2].

To date, 20 chemokine receptors have been identified and particular chemokine receptors are expressed on the surface of hematopoietic cells, endothelial cells, epithelial cells, neurons, and several types of human tumors [1,3]. As for human cancers, Muller et al. [4] demonstrated that two chemokine receptors, CXC chemokine receptor (CXCR) 4 and CC chemokine receptor (CCR) 7, were expressed on the surface of human breast cancer cells and were involved in their metastasis to distant organs that produce and secrete their ligands, CXC chemokine ligand (CXCL) 12, and CC chemokine ligand (CCL) 21. The association between the chemokine–chemokine receptor system and the growth or metastatic potential of ovarian cancer cells, colon cancer cells, pancreatic cancer cells, and human melanoma cells has been reported [5–8].

Concerning the liver, in vitro and in vivo studies showed that hepatocytes, hepatic stellate cells, infiltrating lymphocytes, and hepatocellular carcinoma (HCC) cells express chemokines as well as the respective chemokine receptors, suggesting that the chemokine–chemokine receptor system is involved in the pathophysiology of liver disease including the micro-environment of the tumor [9–12]. However, the role of the chemokine–chemokine receptor system in the tumor biology of HCC remains to be clarified.

* Corresponding author. Fax: +81 75 251 0710.
E-mail address: yitoh@sun.kpu-m.ac.jp (Y. Itoh).

0006-291X/$ - see front matter © 2004 Elsevier Inc. All rights reserved.
doi:10.1016/j.bbrc.2004.07.207

In the present study, we have confirmed the enhanced surface expression of CCR6 on human HCC cell lines and investigated whether chemokine receptor CCR6 and chemokine CCL20 (the specific ligand for CCR6) axis is involved in the biology of human HCC cell lines in vitro.

Materials and methods

Cell lines and HCC tissues. The following human HCC cell lines were used in this study: HLE–JCRB0404, HLF–JCRB0405, HuH7–JCRB0403, PLC/PRF/5–JCRB0406, Chang Liver–JCRB9066 (HSRRB, Osaka, Japan), and HepG2 (Rinken Cell Bank, Tsukuba, Japan). All cell lines were maintained in modified Eagle's medium (Nissui Pharmaceutical, Tokyo, Japan) supplemented with 10% fetal calf serum (Invitrogen, Carlsbad, CA, USA), L-glutamine (Nissui Pharmaceutical), and 20 μg/ml Gentamicin (Sigma Chemical, St. Louis, MO, USA) in a humidified atmosphere of 5% CO_2 at 37 °C. When the experiments were performed, the medium was changed to the new medium containing 1% FCS. HCC tissues were obtained from patients with HCC in accordance with the Declaration of Helsinki. This study was approved by the Ethical Committee of our University.

RNA isolation and reverse transcription. Total RNA was extracted from the cell lines and the HCC tissues using Trizol reagent (Invitrogen) according to the manufacturer's instructions. Then, the RNA preparation was treated with DNAse I (Promega, Madison, WI, USA) to remove residual genomic DNA. One microgram of the RNA was reverse-transcribed using TaqMan Reverse Transcription Reagents (Applied Biosystems, Perkin–Elmer, Foster City, CA, USA) to prepare template cDNA, which was then diluted with sterile water and stored at −20 °C.

Quantitative analysis of mRNA expression in HCC cell lines by real-time polymerase chain reaction (TaqMan). In the preliminary study, quantitative analysis of the mRNA expression of all known chemokine receptors (CCR1–CCR10, CXCR1–CXCR6, XCR, and CXC3R) was performed on each cell line using the fluorescent TaqMan assay. Then, CCR6 was selected because the mRNA expression was in high levels in three cell lines (HuH7, PLC/PRF/5, and HepG2). The primers and probes were either designed using Primer Express software version 1.5 (Applied Biosystems, Perkin–Elmer) or purchased from the Technical Support Section of Applied Biosystems Japan. The following primers were used for CCR6. 5′-CCA TTC TGG GCA GTG AGT CA-3′, 5′-AGC AGC ATC CCG CAG TTA A-3′, and TaqMan probe; CAG CAA TGC CAC GTG CAA GTT GCT A (reference sequence: GenBank Accession No. NM004367). One hundred nanograms of cDNA that had been prepared from each HCC cell line was mixed with TaqMan Universal Master Mix (Applied Biosystems, Perkin–Elmer), 200 nM of gene-specific TaqMan probe, and 900 nM each of gene-specific forward and reverse primers. As an internal positive control, 18S Ribosomal RNA-specific pre-developed TaqMan assay reagent was used. The protocol for the quantitative analysis of chemokine receptor mRNA expression using the ABI Prism 5600 Sequence Detection System (Applied Biosystems, Perkin–Elmer) was as follows: stage 1, 50 °C for 2 min; stage 2, 95 °C for 10 min; and stage 3, 40 cycles of 95 °C for 15 s and 60 °C for 1 min.

To compare the amount of chemokine receptor mRNA in each HCC cell line, we used human peripheral blood cells obtained from a healthy volunteer. Total RNA was extracted from the peripheral blood cells and reverse transcription (RT)-PCR for each chemokine receptor was performed. Then, serially diluted cDNA samples were prepared. For relative quantitation of the target mRNA (chemokine receptor), we used the $\Delta\,\Delta C_T$ calculation described in User Bulletin No. 2 (Applied Biosystems, Perkin–Elmer). The PCR products were subjected to 2.5% w/v agarose gel electrophoresis and stained with ethidium bromide. The PCR products were sequenced with the ABI Prism 377 sequencer to ascertain that the sequence of the PCR product corresponded to the expected sequence.

Flow cytometric analysis of CCR6 expression on HCC cell lines. Cultured HCC cells were washed twice with phosphate-buffered saline (PBS: 10 mmol/L, pH 7.4) and incubated in 1 mM EDTA-PBS containing 1% BSA to detach them from the dishes. Cells were washed twice with PBS containing 1% BSA, and resuspended and adjusted to 1×10^5 cells/ml. After gentle pipetting with a 26G syringe, each sample was treated with human IgG (Chemicon International, Temecula, CA) to block the Fc receptor. To evaluate the surface expression of CCR6 on the HCC cells, cells were incubated at 4 °C for 60 min with the monoclonal antibody against CCR6, or the appropriate isotype control (R&D Systems, Minneapolis, MN, USA) in a dark room. The cells were then washed twice with PBS, and 7×10^3 cells were introduced into a FACScan Calibur (Becton–Dickinson Immunocytometry Systems, San Jose, CA, USA) to investigate the expression of CCR6 on the surface of the cells.

RT-PCR for mRNA expression of chemokine CCL20 (MIP-3α) in HCC cell lines and measurement of their protein concentrations in the culture supernatants. Since chemokine receptor CCR6 was abundantly expressed on the surface of several HCC cell lines, we examined the mRNA expression of their corresponding ligand, CCL20 (MIP-3α), in the HCC cell lines by RT-PCR. The following primers were used for RT-PCR: CCL20 (MIP-3α), 5′-GCT GCT TTG ATG TCA GTG CT-3′, and 5′-TGT CAC AGC CTT CAT TGG C-3′ (reference sequence: GenBank NM004591) and β-actin, 5′-CGG GAA ATC GTG CGT GAC AT-3′ and 5′-GAA CTT TGG GGG ATG CTC GC-3′ [13].

One microliter of the reverse-transcribed product was subjected to PCR amplification using *Taq* polymerase (Toyobo, Osaka, Japan). The conditions of PCR were 35 cycles of 94 °C for 30 s, 50 °C for 30 s, and 72 °C for 30 s. For amplification of the control β-actin, PCR was performed for 25 cycles. The PCR products were sequenced to ascertain that the products corresponded to the expected sequences as already described.

The concentrations of CCL20 in the culture supernatants of HCC cell lines were determined using an enzyme-linked immunosorbent assay (ELISA) kit (R&D Systems) according as the manufacturer's instruction. Data were obtained from duplicate samples in three independent experiments.

Cell growth assays. The effect of CCL20 and PD98059 (a p44/42 MAPK inhibitor) on the proliferation of HuH7 cells and HLE cells was studied. The degree of growth of the cells was evaluated by a colorimetric method utilizing the metabolic dye, 3-(4,5-dimethylthiazol-2-yl)-2,5-diphenyltetrazolium bromide (MTT). In brief, HCC cells (25×10^3 cells/well) were incubated in medium containing 1% FCS with or without various concentrations of CCL20 (MIP-3α) (PeproTech EC, London, UK) or PD98059 (Cell Signaling Technology, Beverly, MA, USA) in 96-well microplates. After incubation for 48 h, the number of viable cells attached to the 96-well microplate was determined using Cell Count Reagent SF (WST-8; Nacalai Tesque, Kyoto, Japan), and the optical density was quantified with a Fluoroscan fluorometer (Multiskan Bichromatic, Labsystems, Helsinki, Finland) at 450 nm. To correct the wavelength, we subtracted the value at 620 nm from that at 450 nm. For each cell line, data were obtained from duplicate samples in three independent experiments.

Western blot analysis. HuH7 cells were incubated with CCL20, and we studied whether there were any changes in the levels of downstream effector proteins in the HuH7 cells. The medium of HuH7 cells (3×10^5 cells/well) that had been maintained in 35 mm dishes was replaced with a new medium containing 1% FCS for 12 h. Then, the medium was changed to new medium containing various concentrations of CCL20 (MIP-3α) (PeproTech EC). After the cells were incubated for 5–60 min, they were lysed in Cell Lytic-MT (Sigma, St. Louis, MO, USA) supplemented with Phosphatase Inhibitor cocktail 2 (Sigma) and Complete Protease Inhibitor cocktail (Roche, Mannheim, Germany). The cell lysates were centrifuged at 15,000 rpm at 4 °C for 5 min. The supernatants were stored as whole cell extracts at −80 °C until use. The protein concentration in the supernatants was measured in triplicate using Bio-Rad protein assay (Bio-Rad Labs, Herculus,

CA, USA). Aliquots (30 μg protein) of the whole cell extracts were subjected to 11% SDS–polyacrylamide gel electrophoresis and then electroblotted onto PVDF membranes (Millipore, Bedford, MA, USA). The total (non-phosphorylated + phosphorylated forms) levels of p44/42 MAPK, p38 MAPK, and stress-activated protein kinase (SAPK/JNK), and the levels of the phosphorylated forms of p44/42 MAPK, p38 MAPK, and SAPK/JNK, were determined by applying the appropriate monoclonal antibodies (Cell Signaling Technology). The blots were developed by an enhanced chemiluminescent detection system (SuperSignal West Pico Chemiluminescent Substrate; Pierce, Rockford, Illinois, USA).

Statistical analysis. All data were expressed as means ± SD. Statistical analyses were performed by ANOVA using the SAS/PC statistical package (SAS Institute, Cary, NC). A p value <0.05 was considered to be statistically significant.

Results

Quantitative analysis of mRNA expression of CCR6 in HCC cell lines by real-time RT-PCR and confirmation of their surface expression on HCC cell lines

In our preliminary study, we performed a comprehensive analysis of the mRNA expression of CCRs and CXCRs in human HCC cell lines using real-time quantitative RT-PCR (data not shown). Among all the known chemokine receptors, three cell lines (HuH7, PLC/PRF/5, and HepG2) especially the HuH7 cells expressed a higher level of CCR6 mRNA whereas HLE and HLF cells expressed negligible levels of CCR6 mRNA (Fig. 1A).

CCR6 was highly expressed on the surface of HuH7, PLC/PRF/5, and HepG2 cells (Fig. 1B), which were the three cell lines that expressed a high level of CCR6 mRNA by RT-PCR (Fig. 1A). Among the studied HCC cell lines, HuH7 cells expressed the highest level of CCR6 on their surface. The surface expression of CCR6 was very low or negligible in HLE, HLF, and Chang liver cells.

mRNA expression of chemokine CCL20 (MIP-3α) in HCC cell lines and their protein concentrations in the culture supernatants

The mRNA expression of CCL20 was demonstrable in three HCC cell lines, HuH7, PLC/PRF/5, and HepG2 cells (Fig. 2A), which were identical with the three HCC cell lines that highly expressed CCR6 on their surface by flow cytometry (Fig. 1B). Interestingly, these three cell lines, especially HuH7, secreted a large amount of CCL20 into the culture supernatant (HuH7, 41,030 ± 5200 pg/ml; PLC/PRF/5, 16,600 ± 3200 pg/ml; and HepG2, 9000 ± 790 pg/ml) during the 48 h culture, suggesting that CCR6–CCL20-mediated signaling pathways may be involved in multiple biological behaviors of these cell lines via paracrine and/or autocrine mechanisms. The concentration of CCL20 in the culture supernatant was low or negligible in the other three cell lines (Fig. 2B).

Influence of the CCR6–CCL20-mediated signaling pathway on the growth of HuH7 cells via phosphorylation of p42/44 MAPK and up-regulation of CCR6 mRNA

To assess the biological behavior resulting from the CCR6–CCL20-mediated signaling pathways in HCC cell lines, we added CCL20 to the culture medium of HCC cell lines and studied the influence of CCL20 on the growth of HCC cells in our preliminary experiments.

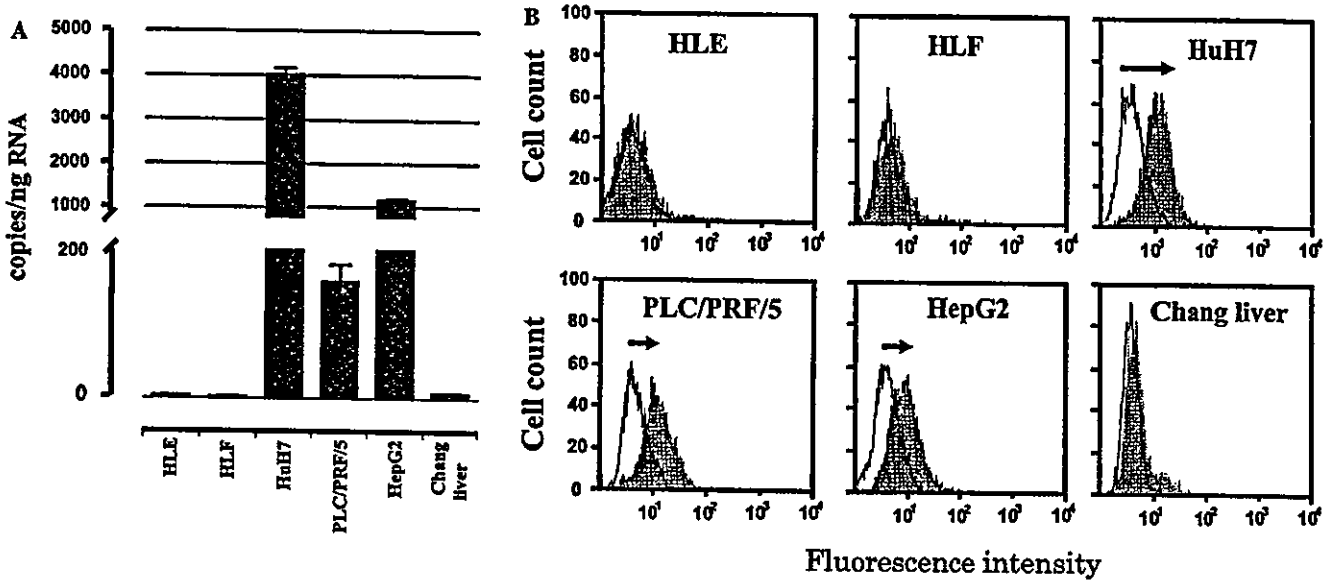

Fig. 1. (A) Quantitative analysis of mRNA expression of CCR6 in five human HCC cell lines and Chang liver cells by real-time RT-PCR (TaqMan). Data are expressed as means ± SD in three independent experiments. (B) Flow cytometric analysis of chemokine receptor CCR6 expressed on the surface of human HCC cell lines. Each cell line was incubated with FITC-labeled anti-human CCR6 antibody. Representative results are shown. shaded histogram: FITC-labeled CCR6 antibody, unshaded histogram: isotype-specific mouse IgG.

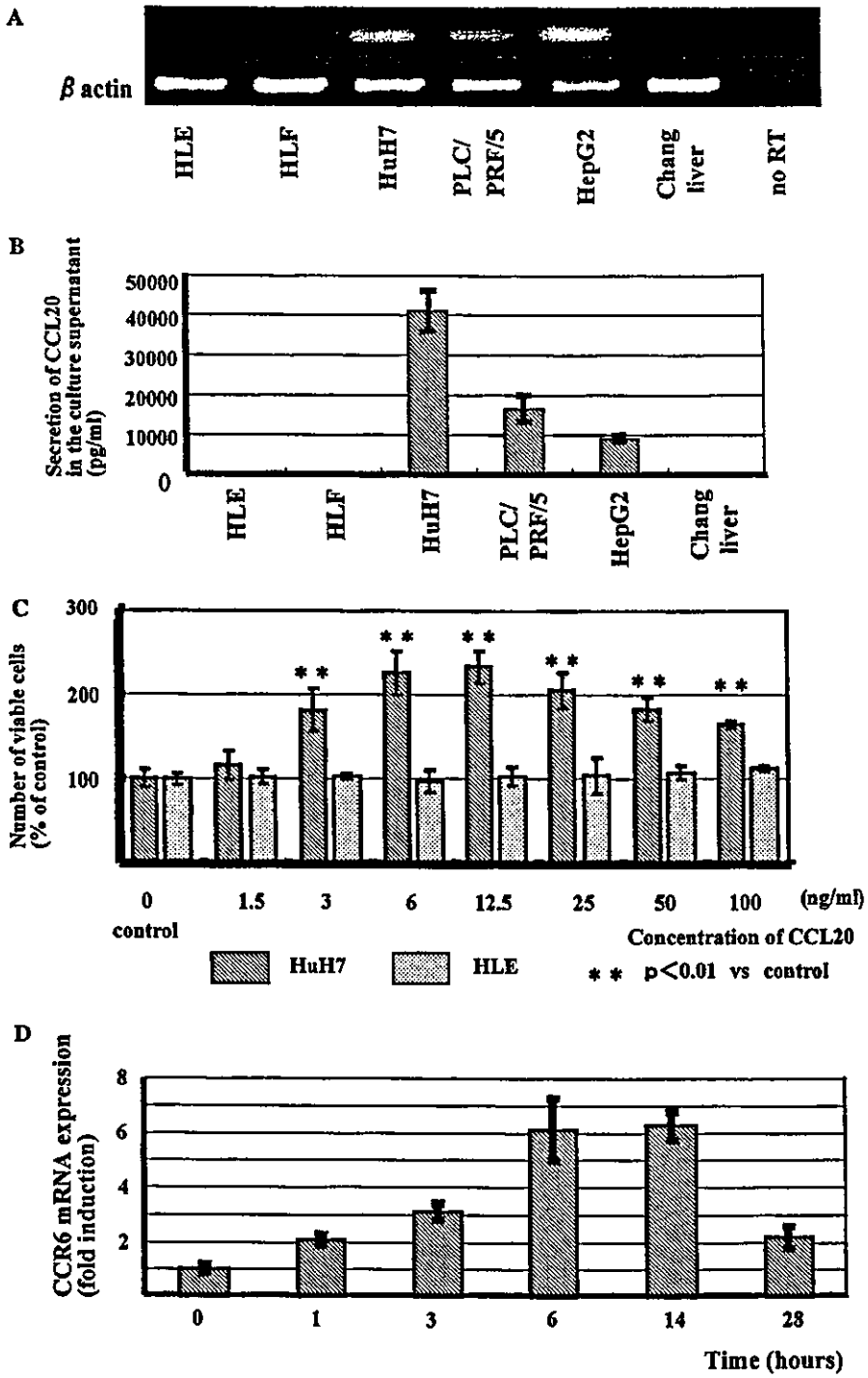

Fig. 2. (A) RT-PCR analysis for the mRNA expression of CCL20 (MIP-3α), the ligand of CCR6. (B) The concentrations of CCL20 in the culture supernatants of HCC cell lines. Cells (5×10^5 cells/500 μl) were incubated in 24-well microplates for 48 h, and the concentrations of CCL20 in the culture supernatants were determined by ELISA. Data (means ± SD) are obtained from duplicate samples in three independent experiments. (C) The number of viable HuH7 cells and HLE cells after incubation with CCL20 for 48 h was determined by the MTT assay. Control cultures were incubated in the absence of CCL20. Data (means ± SD) were obtained from duplicate samples in three independent experiments. (D) Real-time RT-PCR for CCR6 mRNA expression at the indicated time points in HuH7 cells that were stimulated with 100 ng/ml of CCL20. Data were shown as means ± SD of three independent experiments. PCR analysis in each experiment was carried out in triplicate.

As the results, CCL20 promoted the growth of CCR6-expressing HuH7, PLC/PRF/5, and HepG2 cells, and most prominently the HuH7 cells (data not shown).

When HuH7 cells were stimulated with various concentrations of CCL20 for 48 h, CCL20 at a concentration as low as 3 ng/ml significantly promoted the

growth of HuH7 cells (Fig. 2C). CCL20 enhanced the growth of HuH7 cells by the greatest degree at a concentration of 12.5 ng/ml (by approximately 220%; $p < 0.01$). CCL20 did not induce the growth of HLE cells, which expressed a negligible level of CCR6 on their surface by flow cytometry.

Interestingly, the addition of CCL20 to the culture medium of HuH7 cells enhanced the expression of CCR6 mRNA at 1 h and continued to increase the expression up to 14 h, implying that the CCR6–CCL20 axis had a positive feedback up-regulation loop for CCR6 mRNA (Fig. 2D).

Next, we studied whether the CCR6–CCL20 axis actually affected intracellular signaling pathways. When HuH7 cells were treated with CCL20, the level of phospho-p44/42 MAPK increased in a time-dependent manner, and activation of p44/42 MAPK continued through 60 min (Fig. 3A). When HuH7 cells were pretreated with a p44/42 MAPK inhibitor (PD98059) 30 min before the addition of CCL20, the CCL20-induced activation of

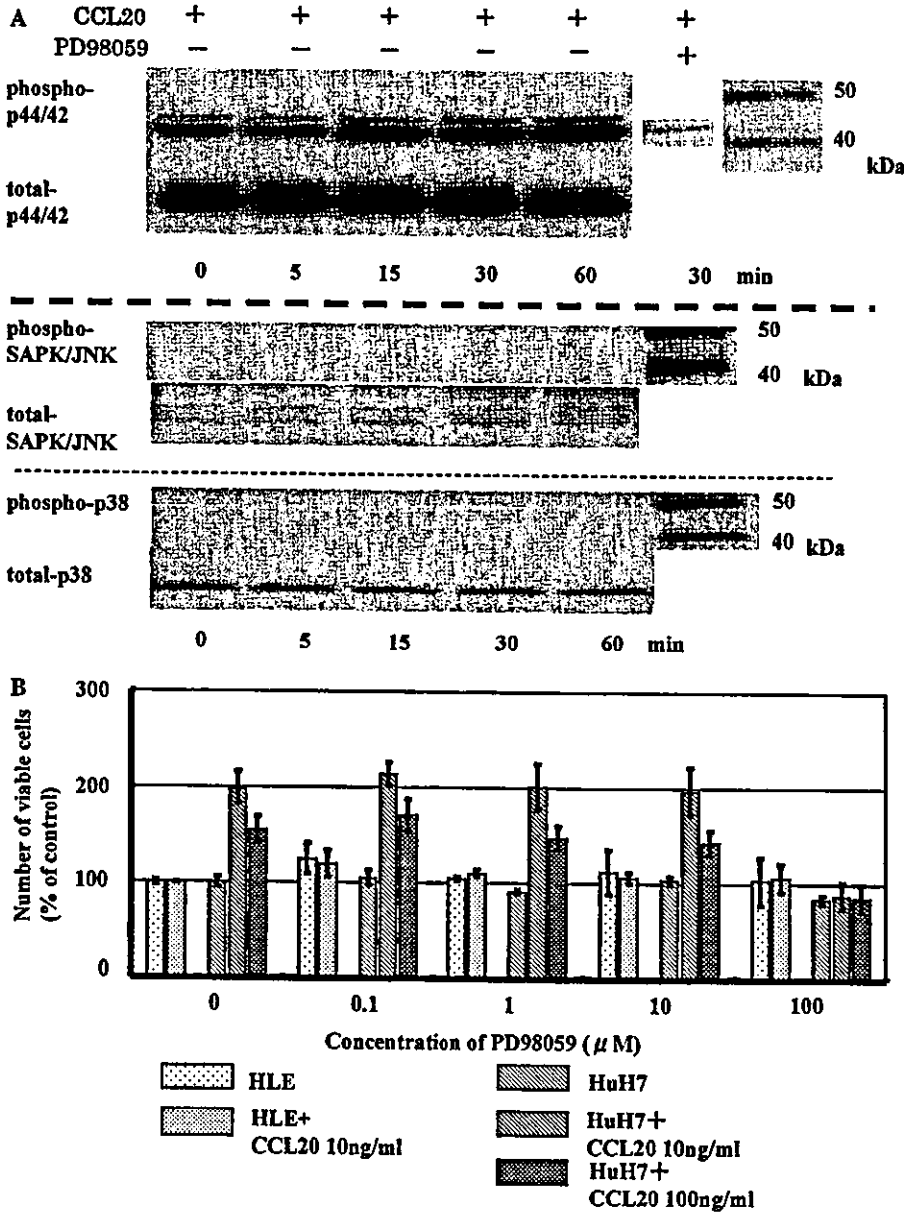

Fig. 3. (A) Western blot analysis of p44/42, SAPK, p38, and the phosphorylated forms of p44/42, SAPK, and p38 in HuH7 cells that were stimulated with 100 ng/ml CCL20 for the indicated time intervals. Total cell lysates were immunoblotted with antibodies specifically recognizing each protein. Some cells were pretreated with MEK 1/2 inhibitor (PD98059) for 30 min before the addition of CCL20. (B) Number of viable HuH7 cells and HLE cells that were stimulated with CCL20 for 48 h in the presence of various concentrations of PD98059, a p44/42 MAPK inhibitor. The number of viable cells was evaluated by the MTT assay. Data were expressed as the percentage of that in the control cultures that had not been treated with CCL20 nor PD98059 (%). Data are shown as means ± SD of three independent experiments.

p44/42 MAPK was inhibited. The p38 MAPK and SAPK/JNK cascades were not active before nor after stimulation with CCL20, which indicated that the CCR6–CCL20 axis may have solely activated p44/42 MAPK to promote the growth of HuH7 cells.

To confirm that p44/42 MAPK activation is required for CCL20-dependent proliferation of HuH7 cells, we examined the growth of HuH7 cells in the presence of PD98059 (Fig. 3B). Cells were treated for 48 h with CCL20 (10 or 100 ng/ml) in the presence or absence of various concentrations of PD98059. CCL20-induced growth of HuH7 cells was inhibited by pretreatment with PD98059 at the concentration of 100 μM, whereas the growth of HLE cells, which expressed negligible levels of CCR6, was not affected by the pretreatment of PD98059.

Detection of CCR6 mRNA in HCC

The expression of CCR6 mRNA in human HCC tissues was analyzed by TaqMan PCR. The mRNA of CCR6 was detectable in 19 of the 26 HCC samples, although the expression level varied among the samples. There was no relationship between the level of CCR6 mRNA expression and the degree of differentiation of HCC (data not shown).

Discussion

CCL20 (MIP-3α) is expressed by activated cells including monocytes, T cells, dendritic cells, endothelial cells, and fibroblasts, while CCR6 is expressed in the liver, lungs, and some lymphoid tissues [2,3,14,15]. Inflammatory cytokines such as tumor necrosis factor alpha (TNF-α), interleukin 1β (IL-1β), interferon-γ (IFN-γ), CD40 ligand, and interleukin 17 (IL-17) induce CCL20 expression [16], and several experimental evidences indicate that the CCL20–CCR6 axis has many physiologic or pathobiological functions [17,18]. For example, the interaction between CCL20 and its receptor CCR6 was demonstrated to be important for recruitment of T cells to lesional psoriatic skin [18].

Concerning cancer biology, several types of tumor cells express chemokines to up-regulate their own growth [3]. Formerly, Kleeff et al. [19] reported that pancreatic cancer cell lines overexpressed CCL20, which contributed to their own growth and invasion. However, the direct contribution of the CCL20–CCR6 axis in the tumor biology of HCC, such as tumor cell growth and invasion, has not been examined.

In the present study, we found that chemokine receptor CCR6 was highly expressed on the surface of three human HCC cell lines, i.e., HuH7, PLC/PRF/5, and HepG2 cells (Fig. 1B). In our preliminary study, we examined the effect of CCL20 on the chemotaxis of HCC cell lines HuH7, PLC/PRF/5, and HepG2, all of which express CCR6 on their surface, using the invasion chamber; however, CCL20 did not have a significant effect on the chemotaxis of these cells (data not shown). On the other hand, the MTT assay demonstrated that CCL20 enhanced the growth of HuH7 cells between 3 and 12.5 ng/ml in a concentration dependent manner. Interestingly, three cell lines (HuH7, PLC/PRF/5, and HepG2), which expressed high levels of CCR6 on their surface, secreted CCL20 into the culture supernatant. In particular, HuH7 cells secreted a significant amount of CCL20 (Fig. 2B). These results suggest that a CCL20–CCR6 autocrine and/or paracrine loop may be involved in the growth of HuH7 cells.

Chemokine receptors are seven-transmembrane, G protein-coupled receptors. After the binding of a chemokine to its chemokine receptor, the signaling pathway leads to the activation of MAP kinases, which comprise a family of serine/threonine kinases including three-tiered cascades, p44/42 MAPK, p38 MAPK, and SAPK/JNK. Several studies have reported that MEK1 and/or p44/42 was phosphorylated when chemokines bound to their receptors [20,21]. Our data in the current study indicated that CCL20 induced the phosphorylation of p44/42 MAPK, but not p38 MAPK or SAPK/JNK, in HuH7 cells (Fig. 3A). In addition, CCL20-induced phosphorylation of p44/42 MAPK was inhibited by PD098059, a MEK inhibitor. PD98059 also inhibited the growth of HuH7 cells that were cultured in the presence of CCL20 (Fig. 3B). These results indicate that activation of the p44/42 MAPK pathway may be associated with the growth of HuH7 cells [22]. This finding is interesting because p44/42 MAPK is known to be phosphorylated by several growth factors such as epidermal growth factor (EGF) [23].

We also demonstrated that CCL20 enhanced the mRNA expression of CCR6 in a time-dependent manner in HuH7 cells (Fig. 2D). Although the mechanism of internalization and recycling of CCR6 was not characterized, CCL20 increased the phosphorylation of p44/42 MAPK, and this may have induced the feedback up-regulation of CCR6 mRNA through some intracellular signaling including p44/42 MAPK.

In summary, the present findings demonstrated that: (1) certain human HCC cell lines expressed a high level of CCR6 on their surface, and these cell lines secreted significant amounts of the respective chemokine CCL20; (2) CCL20 enhanced the growth of HuH7 cells, which expressed a high level of CCR6; (3) a downstream signal transduction pathway of CCL20–CCR6 in HuH7 cells was mediated by p44/42 MAPK, but not by p38 MAPK or SAPK/JNK; and (4) a proportion of human HCCs also expressed CCR6 mRNA. These results indicate that the growth of some human HCC cells may be, in part, mediated by CCL20–CCR6 axis in an autocrine or paracrine manner.